AD-A185 669 TORSIONAL ELASTIC PROPERTY MEASUREMENTS OF SELECTED ORTHODONTIC ARCHWIRES(U) AIR FORCE INST OF TECH WRIGHT-PATTERSON AFB OH B E LARSON 1987 1/1

UNCLASSIFIED AFIT/CI/NR-87-40T F/G 11/6 1 NL

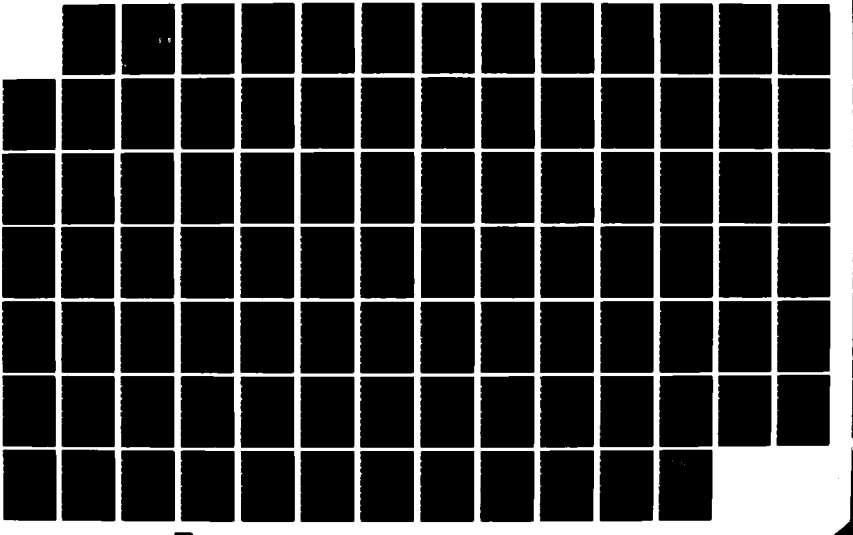

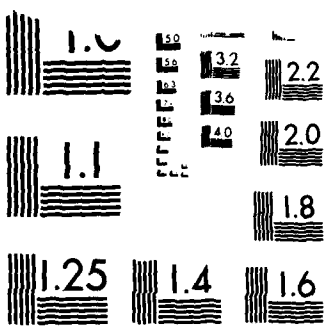

MICROCOPY RESOLUTION TEST CHART

NATIONAL BUREAU OF STANDARDS-1963-A

UNCLASSIFIED
SECURITY CLASSIFICATION OF THIS PAGE *(When Data Entered)*

REPORT DOCUMENTATION PAGE		READ INSTRUCTIONS BEFORE COMPLETING FORM
1. REPORT NUMBER AFIT/CI/NR 87-40T	2. GOVT ACCESSION NO. AD-A185 669	3. RECIPIENT'S CATALOG NUMBER
4. TITLE *(and Subtitle)* Torsional Elastic Property Measurements of Selected Orthodontic Archwires		5. TYPE OF REPORT & PERIOD COVERED THESIS/DISSERTATION
		6. PERFORMING ORG. REPORT NUMBER
7. AUTHOR(s) Brent E. Larson		8. CONTRACT OR GRANT NUMBER(s)
9. PERFORMING ORGANIZATION NAME AND ADDRESS AFIT STUDENT AT: University of North Carolina		10. PROGRAM ELEMENT, PROJECT, TASK AREA & WORK UNIT NUMBERS
11. CONTROLLING OFFICE NAME AND ADDRESS AFIT/NR WPAFB OH 45433-6583		12. REPORT DATE 1987
		13. NUMBER OF PAGES 84
14. MONITORING AGENCY NAME & ADDRESS*(if different from Controlling Office)*		15. SECURITY CLASS. *(of this report)* UNCLASSIFIED
		15a. DECLASSIFICATION/DOWNGRADING SCHEDULE

16. DISTRIBUTION STATEMENT *(of this Report)*

APPROVED FOR PUBLIC RELEASE; DISTRIBUTION UNLIMITED

DTIC ELECTE NOV 0 4 1987 S D

17. DISTRIBUTION STATEMENT *(of the abstract entered in Block 20, if different from Report)*

18. SUPPLEMENTARY NOTES

APPROVED FOR PUBLIC RELEASE: IAW AFR 190-1

Lynn Wolaver 5 Oct 87

LYNN E. WOLAVER
Dean for Research and
Professional Development
AFIT/NR

19. KEY WORDS *(Continue on reverse side if necessary and identify by block number)*

20. ABSTRACT *(Continue on reverse side if necessary and identify by block number)*

ATTACHED

DD FORM 1 JAN 73 1473 EDITION OF 1 NOV 65 IS OBSOLETE

SECURITY CLASSIFICATION OF THIS PAGE *(When Data Entered)*

ABSTRACT

BRENT E. LARSON. Torsional Elastic Property Measurements of Selected Orthodontic Archwires. (under the direction of ROBERT P. KUSY)

A method for quantifying the torsional elastic properties of orthodontic archwires was investigated. Three wire sizes (.018", .017"x.025", and .019"x.025") were tested for three different alloys: stainless steel [S.S.], beta titanium [ß-Ti], and nickel-titanium [Ni-Ti]. The shear modulus (G) was determined dynamically using a torsion pendulum. The torsional yield strength (τ_{ys}) was determined using a static torsion test that generated torque (T) versus angular deflection (ϕ) tracings. The three basic torsional elastic properties (strength, stiffness, and range) were calculated for each of the wires from G, τ_{ys}, and precise dimensional data.

The Ni-Ti wire had the greatest range and the least stiffness. S.S. archwire showed the greatest stiffness and the least range. The properties of ß-Ti fell midway between S.S. and Ni-Ti. The rectangular Ni-Ti wire exhibited some apparent pseudoelastic behavior which resulted in low τ_{ys} results and a wide range of G.

MASTER'S THESIS

TORSIONAL ELASTIC PROPERTY MEASUREMENTS OF SELECTED ORTHODONTIC ARCHWIRES

by

Brent E. Larson, D.D.S.

Advisor

Dr. Robert P. Kusy

Readers

Dr. H. Garland Hershey

Dr. Robert R. Reeber

TORSIONAL ELASTIC PROPERTY MEASUREMENTS

OF

SELECTED ORTHODONTIC ARCHWIRES

by

Brent E. Larson, D.D.S.

A Thesis submitted to the faculty of
University of North Carolina at Chapel Hill
in partial fulfillment of the requirements for
the degree of Master of Science in the
Department of Orthodontics.

Chapel Hill

1987

Approved by:

advisor

reader

reader

ACKNOWLEDGEMENTS

To my wife, Cindy, whose love, patience, and support allowed this educational experience.

To my sons, Matthew and Andrew, who kept everything in its proper perspective.

To Robert P. Kusy, who provided the initial idea and subsequent stimulation for this project.

To H. Garland Hershey and Robert R. Reeber for their time and constructive ideas.

To John Q. Whitley, for the software and technical support.

And finally, to William R. Proffit for giving me the opportunity to study orthodontics and for emphasizing the "Pooh Bear" logic that helped in problem solving.

TABLE OF CONTENTS

LIST OF TABLES

LIST OF FIGURES

CHAPTER 1

INTRODUCTION

Until recent times, stainless steel (S.S.) has been the material of choice for orthodontic archwires since replacing gold in the middle of the century. If the orthodontist wished to have lighter forces over a greater range, he had two choices. First, he could use a smaller cross-section wire. Because the modulus of elasticity of S.S. was so high, the wire had to be small enough to have the appropriate stiffness and range. By that point, the strength wasn't sufficient to stand the forces of mastication and the bracket engagement was not good, a fact that ultimately led to the smaller edgewise bracket slot and the development of multi-stranded stainless steel archwires. The other way to adapt stainless steel for less stiffness and greater range was to fabricate an appropriate loop in the wire. Because stiffness is inversely related to the cube of the length, this was quite functional for first and second order activations where even a small loop would add significant flexibility. Modern edgewise orthodontic appliances utilize torsional energy stored in square or rectangular archwires to perform third order (torquing) tooth movements. It is at best difficult to design a loop for third order flexibility, and less advantageous since stiffness is simply proportional to the

inverse of the length. The orthodontist was forced to make torque adjustments in small increments with a large, torsionally stiff, stainless steel wire.

The concept of variable modulus orthodontics was originally described by Burstone[1] when archwires made of titanium alloys and multi-stranded stainless steel became available. Although the original description focused on first and second order wire activation, variable modulus orthodontics is particularly well suited to third order activation because applied moments may be varied while maintaining an archwire size which is sufficient for full bracket engagement. The utilization of alloys with differing elastic properties necessitates quantification of those properties in order to properly select an archwire for a given situation. Recent research into the elastic properties of orthodontic archwires has focused on testing in tension and bending. Few references addressing the torsional properties of orthodontic wires appear in the literature, and none describe the basic mechanical properties of shear modulus (G) and torsional yield strength (τ_{ys}) for contemporary alloys.

NOTATION

The following symbols will be used throughout the text, tables and figures:

A - The first constant in the geometric regression equation.

b - Smallest cross-sectional dimension of a rectangular wire.

B - The second constant in the geometric regression equation.

d - Diameter of a round wire.

E - Modulus of elasticity, Young's modulus.

EPR - Elastic property ratio.

G - Shear modulus, modulus of rigidity.

h - Largest cross-sectional dimension of a rectangular wire.

I - Mass moment of inertia of a wire about its neutral axis.

I_{mass} - Polar mass moment of inertia.

J - Polar area moment of inertia.

JEL - Johnson Elastic Limit.

k_1 - Shape factor for equation 5.

L - Test length, distance between the clamps.

ΔL - Length correction.

Ni-Ti - Nickel-titanium alloys.

P - Period of oscillation.

r - Coefficient of correlation.

S.S. - Stainless steel alloys.

T - Torque.

T_{Max} - Maximum torque.

v - Poisson's ratio.

β-Ti - Beta titanium alloys.

σ_{ys} - Tensile yield strength.

τ_{ys} - Torsional yield strength.

τ_{Max} - Maximum shear stress.

ϕ - Angular deflection.

μ - Shape factor for equation 3.

LITERATURE REVIEW

PHYSICAL PROPERTIES IN BENDING AND TENSION

The physical properties of elastic modulus (E) and yield strength (σ_{ys}) are needed to describe elastic properties for bending. These properties have been determined both in tension and in a variety of bending modes. Theoretically, the values of E and σ_{ys} should be the same in tension and bending.

Practically, there has not been agreement in the literature on the modulus of S.S. Although studies by Kusy et al[2,3,4] supported the accepted engineering values of 28-29 Msi, Asgharnia and Brantley,[5] Yoshikawa et al,[6] Goldberg et al,[7] and Drake et al[8] reported values of at least 20% less. Those that reported the lower values attributed this difference to the severe cold drawing of the orthodontic wire and assumed the lower values were correct. However, they were unable to demonstrate any preferred crystal orientation by x-ray experiments.[7] Until there is some definite evidence to the contrary, it must be assumed that the correct values are those approximating the engineering values, and that the consistently low values are due to some systematic experimental error.

Yield strength values for S.S. are more difficult to

compare because of their susceptibility to cold-working and heat treatments. Most values are reported in the range 100-280 ksi.[2,4,5]

Modulus and yield strength values for beta-titanium (ß-Ti) have been reported in two recent studies. Asgharnia and Brantley[5] reported modulus values from 11.5 to 13.8 Msi determined in cantilever bending and σ_{ys} values of 140-190 ksi in tension. Kusy and Stush[9] found that E equalled 10.5 Msi in 3- and 4- point bending, and that σ_{ys} equalled 76-98 ksi in tension.

The physical properties, E and σ_{ys}, were also described for nickel-titanium (Ni-Ti) in the above two studies. Kusy and Stush found the modulus was 6.44 Msi for round but only 4.85 Msi for square and rectangular wires. They also reported that the 0.1% yield strength decreased as a function of increasing cross-sectional area, ranging from 45-122 ksi. Asgharnia and Brantley reported values of E from 5.5-7.6 Msi and σ_{ys} values from 57-100 ksi.

ELASTIC PROPERTY COMPARISONS

Burstone developed the concept of wire stiffness numbers (W_s) to allow comparison of orthodontic wires. The concept of W_s is based on the engineering relationship,

Stiffness = Elastic Modulus(E) x Moment of Inertia(I).

He attempted to simplify this for the clinician by defining the material stiffness (M_s) as 1.0 for stainless steel and related all others to that normal value. He also defined the cross-sectional stiffness (C_s) which normalized the values of I to a baseline of 0.004" round wire. The relationship that then resulted was,

$$W_s = M_s \times C_s.$$

This allowed the practitioner to compare wire stiffness by knowing the material and cross-sectional configuration.

In order to consider the other two basic elastic properties of strength and range, along with stiffness, Kusy and Greenberg[10] used a system of elastic property ratios (EPR's). The EPR's are an extension of Thurow's comparisons for cross-sectional configuration differences,[11] which allow for compositional differences as well.

TORSIONAL TESTING

Even though ADA specification No. 32 for Orthodontic wires[12] makes no testing requirements for wires in torsion, three approaches have been previously described to determine the torsional response of orthodontic archwires: 1), <u>in vitro</u> dentition model; 2), theoretical calculation; and 3), static torsional measurements.

An in vitro dentition model attempts to duplicate the tooth to tooth relationships found in the mouth on a bench-top model. This model can then be used to measure the effects and side-effects of a particular appliance set-up.

Such a study by Steyn[13] used a phantom head with an acrylic maxilla in a study that measured the palatal root torque applied to anterior teeth by edgewise, 0.021x 0.025" stainless steel archwires. The forces exerted at the alveolar crest and apex of the incisors (9 and 18 mm from the bracket slot, respectively) were measured with strain gauges. The expected linear relationship between the torque magnitude and the activation angle was verified.

More recently, Wagner and Nikolai[14] used a dentition model to study torsional stiffness in incisor segments using a variety of archwire configurations, wire sizes, and wire materials. Their model was constructed to a Bonwill-Hawley arch form, and had rigid posterior segments together with individual acrylic incisors. A force couple was placed on the incisors by means of monofilament lines and weight buckets. It served to revolve the incisors around the archwire. The teeth were rotated on S.S. and chrome-cobalt wires with maximum moments of 2800-4300 gm-mm resulting in angular deflections of 20-45 degrees. None of the archwires tested showed any measurable permanent set at these levels of activation. They reported mean torsional stiffness in gm-mm per degree, and concluded that,

"torsional behavior is associated with the elastic shear modulus," but they made no attempt to quantify that value.

Theoretical calculations of EPR's were completed by Kusy et al[10,15] for a variety of wire sizes, shapes, and types. Beginning with standard engineering equations that describe elastic behavior; strength, stiffness, and range ratios were computed for bending and torsion based on wire dimensions and physical properties. Fifty-four elastic property ratio formulas resulted, and tables were presented that allowed comparison of two archwires if the cross-sectional dimensions and physical properties were known. The shortcoming of this work was that the values of G and τ_{ys} had to be estimated for most materials. Experimental verification of these values is needed before the elastic property ratios they calculated can be accepted as accurate.

Historically, the static torsional test method has been accepted for the torsional testing of metals.[16,17,18,19] The general procedure for such a test is to clamp a test specimen at both ends in an apparatus that keeps the clamps and specimen coaxial during rotation. One clamp is then rotated while the other is fixed and a record is made of the torque produced for various amounts of angular deflection. G and τ_{ys} can be determined from this information.

The static torsion test has been used infrequently to

determine torsional elastic properties of orthodontic wires. Andreasen and Morrow[20] compared stainless steel to Nitinol (nickel-titanium) using this method. They clamped a specimen between a fixed jaw and a rotating jaw with a gauge length of 1". The torsional moment was measured as a function of the torque angle through 720 degrees (2 complete revolutions). The wire was then allowed to return to a neutral position and the permanent set recorded. The authors stated that, "The most important benefits from Nitinol wires are realized when a rectangular wire is inserted early in treatment." They further stated that, "...torquing can be accomplished earlier with a resilient rectangular wire, such as Nitinol." Nitinol was found to develop a lower torsional moment and exhibit less permanent set than stainless steel under the same conditions.

Zimmerman[21] described a limited torsional comparison of Nitinol and stainless steel archwires. He constructed a custom test apparatus which consisted of a gear box and chuck at one end, to deliver and measure the input rotation, and a chuck mounted to a torque gauge on the other end. A 1" gauge length was used, and the gauge end was free to move axially in order to compensate for length changes during rotation and to avoid any axial strain. He realized the need to correct for gauge deflection and included that in his results. Nitinol samples were found to be about 4.5 times less rigid and to have 2.5-3.0 times

greater range than the stainless steel alternatives.

Drake et al[8] evaluated the torsional properties of a stainless steel, a nickel-titanium, and a titanium-molybdenum (beta titanium) alloy. They used a gauge length of 10 mm in a commercially available instrument that measured torsional moment as a function of torsional angle. The specimens were rotated at a rate of 2 revolutions per minute up to 90 degrees. The stiffness was reported as a spring rate, which was the slope of the straight-line portion of the moment-deflection curve. Results showed that nickel-titanium wires had a spring rate about one-fourth that of stainless steel and one-half that of titanium-molybdenum.

Nederveen and Tilstra[22] described a source of error which occurs when simple theory is applied to torsion testing. Theoretically, the amount of twist for a given torque should be proportional to length. Practically, when rotating clamps are used for testing and the distance between the clamps is used as the specimen length, errors result. This error may be the result of warping or deformation of the material enclosed by the clamp. An experimental method for correction of these errors was introduced as a length correction (ΔL) which was added to the inter-clamp distance when the shear modulus was calculated. This correction becomes more important as the specimen length is reduced and ΔL becomes a greater

proportion of the gauge length.

DYNAMIC TORSION TESTING

The shear modulus of materials can also be determined by using dynamic methods. Many types of dynamic tests have been described which measure the response of a material to time dependent stresses: free vibration, forced vibration, and pulse propagation. The simplest of these tests, the torsion pendulum, has often been used to describe the torsional properties of materials. In this test, one end of the specimen is rigidly fixed while the other end is clamped to a freely movable moment of inertia member. When the inertia member (or pendulum) is twisted and released, the system will oscillate with a characteristic periodicity. While the period of oscillation remains constant, the amplitude will decrease with time.

Nielsen[23] has proposed such an apparatus to measure the stiffness and damping characteristics of high polymers. A design was described with the pendulum hanging freely beneath the specimen. This put axial stress on the specimen and tended to reduce the period of oscillation. In order to calculate the period at zero tension, the tests were run at a series of known tensions. When a plot of $1/\text{period}^2$ versus tension was made, the results extrapolated to zero tension.

Neilsen[24] also described a recording pendulum which

allowed for a continuous record of pendulum motion. This device was designed in an inverted configuration so that the pendulum was suspended above the specimen with a fine wire. This avoided putting tension on the specimen and allowed direct measurement of the period. He claimed the torsion pendulum could be used over a wide range of shear modulus values (from about $3x10^6$ to over 10^{11} dynes/cm^2), frequencies (0.05-5 cycles per second), and damping. Because of the low stresses induced during testing, the value of G was reported to be independent of the angle of twist. Neilsen also found that the largest errors in pendulum tests were made in measuring specimen dimensions.

Heijboer[25] has also used an inverted, or counterbalanced, torsion pendulum for testing polymers. He performed classic experiments in which substituent groups were systematically changed to understand the effects of structure on the dynamic mechanical properties of macromolecules. He stated that, "the conventional torsion pendulum is unsurpassed in accuracy and reliability (and that) the absolute modulus can be obtained with an accuracy of at least 2%."

One study in the dental literature used a torsion pendulum to investigate the viscoelastic properties of denture base acrylics.[26] In this experiment, an inverted pendulum was hung by a fine, fixed wire. The amplitude and frequency of oscillation were monitored by a lamp

reflecting off of a mirror which had been attached to the inertia assembly. Their results were consistent with modulus data obtained by a static method.

PURPOSE

The orthodontist requires information on the torsional properties of various alloys in order to make informed decisions for routine patient treatment. Consequently, methods for determining G and τ_{ys} were investigated, and the elastic properties of three alloys were described.

CHAPTER 2

MATERIALS AND METHODS

TEST SPECIMENS

Three alloys were selected for this investigation (Table I): stainless steel (S.S.), beta titanium (ß-Ti), and nickel-titanium (Ni-Ti). Each alloy was tested in three cross-sectional configurations: .018" round, .017x.025", and .019x.025". All wires were obtained in straight lengths except the .018" Ni-Ti, which was available only in preformed arches. The round wires were included not only because they may be torsionally activated in some torquing auxiliaries, but primarily because they provided a control to evaluate the empirical equations used for rectangular cross-section samples.

CROSS-SECTIONAL WIRE DIMENSIONS

Actual wire cross-sectional dimensions were measured to the nearest 0.00005" with a digital micrometer*. For round wires the diameter (d) was measured. The rectangular wires required two measurements to define the cross-section: base (b), and height (h). Figure 1 shows the measurements made. Each wire specimen was measured at

---

* Sony µ-Mate, M-2030, National Machine Systems, Inc., Tustin, CA.

three spots along the test span. The three values were then averaged and the mean was rounded to the nearest 0.00005".

LOAD CELL CALIBRATION

All tests used a 2,000 kg-cm torsional load cell to measure the torque applied to specimens. The small magnitude of the torques measured in this experiment necessitated amplifying the output 5 times beyond its usual most sensitive scale (5 kg-cm). The result was a full scale reading of 1 kg-cm. The load cell was electronically calibrated before each testing session. In addition, the following procedure was done prior to any testing to verify the accuracy and linearity at this amplification.

A device was fabricated that had a precise 10 cm. moment arm when inserted into the load cell chuck. Precision weights were then hung from the end of the arm with the load cell mounted parallel with the floor. The moment applied was calculated by the equation,

$$\text{moment applied (kg-cm)} = \text{mass of weight (kg)} \times 10 \text{ cm.} \quad (1)$$

Moments were applied from 0.1 - 1.0 kg-cm in increments of 0.1. The moments applied were checked against the load

cell output to verify accuracy and linearity. To verify that load cell position did not effect this test, the load cell was mounted perpendicular to the floor (test position) and the test repeated. Because of the 90 degree position change, this time the weights were hung by a monofilament line over a low friction pulley.

SHEAR MODULUS

To measure the shear modulus an attempt was first made with a static torsion apparatus. An Instron Universal Testing Machine* was equipped with a 2,000 kg-cm load cell and torsion testing fixture. Testing of the apparatus was done first with relatively large, 0.090", specimens of steel and aluminum. After correcting for clamping errors, values of shear modulus (G) were obtained which were comparable with the literature, but not without a great deal of variability. When the same procedure was used for orthodontic archwires specimens, there was once again a great deal of variability. The static torsion method for modulus determination was abandoned in favor of the torsion pendulum (cf. Appendix A for further information on preliminary static torsion tests).

The torsion pendulum was selected for use in this study after verification of the method on samples of carbon steel, stainless steel, brass, and copper (cf. Appendix B

---

* Instron Corporation, Canton, MA.

for details). A torsion pendulum was designed and constructed so that the polar mass moment of inertia (I_{mass}) could be easily and rapidly changed without removing the specimen from the clamps by removing one nut, "A" (Figure 2). This was done with a modular design that separates the clamping component, "B", from the disk component that provides the majority of the inertia,"C". Interchangeable disks of brass and aluminum were made to allow values of I_{mass} ranging from 43 to 13,543 gm-cm^2. The actual clamping of the wire specimens was done with small, four-jawed, pin vises*, "D".

The shear modulus (G) was determined dynamically using this torsion pendulum mounted on an Instron Universal Testing Machine** with a 2,000 Kg-cm torsional load cell. The load cell was used as the fixed end of the pendulum apparatus and provided a continuous output of the torsional stresses on the specimen and therefore a measurement of the amplitude and frequency of pendulum motion. The pendulum was twisted and released, causing the system to freely oscillate, and the sinusoidal load cell output was collected digitally. A Commodore 64 computer, interfaced to the Instron machine through an analog to digital (A-D) converter was used as a data buffer to collect and store the raw data. The custom software for the Commodore

---

* The L. S. Starrett Co., Athol, MA.

** Instron Corporation, Canton, MA.

allowed the selection of data sampling rate, as well as input monitoring and diskette storage functions. The data was collected at approximately 125 data points per second to allow generation of smooth sinusoidal output curves. After the testing was done, the digital data was transferred to an IBM PC/XT for analysis. A basic software program called <PENDULUM> allowed calculation of the period of oscillation (P) and G by positioning cursors on the screen and entering dimensional information when prompted. The first five complete oscillations were used to determine P. Figure 3 shows the computer screen for <PENDULUM> with the cursors placed. In cases where five were not available, the maximum number of complete oscillations displayed was used.

The <PENDULUM> software incorporated the relationships given by Nielsen[23] to determine G:

for circular cross sections,

$$G(psi) = \frac{3.550 \times 10^{-4}}{d^4 P^2} I_{mass} L \quad , \quad (2)$$

and for rectangular cross sections,

$$G(psi) = \frac{5.588 \times 10^{-4}}{hb^3 \mu P^2} I_{mass} L \quad , \quad (3)$$

where I_{mass} was in gm-cm^2, L was the wire specimen length (in.), μ was a shape factor (Table II), and d, b, and h were wire dimensions (in.). Wire specimen lengths of 2 in.

were measured to the nearest 0.001" with a dial caliper*. These corresponded to the longest straight segment of the preformed arches.

Since eqs. 2 and 3 assume a value of P with no tension on the specimen, two different pendulum configurations were used to determine P at zero tension.

In the first method, three samples of each wire size and configuration were tested on an inverted pendulum. The pendulum was positioned above the specimen balanced so the weight of the pendulum was opposed by a counterweight connected over a pair of pulleys (Figure 4). For each wire type and size, five values of I_{mass} were selected that allowed for P to be between 0.5 and 1.5 seconds. Table III shows the inertias used for each wire size and type. Each specimen was run five times using the five different values of I_{mass} (Figure 5).

For the second method, a hanging pendulum was used to determine G. The pendulum was suspended freely below the specimen with a hook placed so that weights could be suspended from the pendulum (Figure 6). The same three wire samples for each size and type were used, and each was tested at a series of five known tensions. <PENDULUM> was used to determine P and a linear regression of $1/P^2$ versus tension was done for each sample (Figure 7). The y-intercept gave the value of $1/P^2$ at zero tension, and eqs.

---

* The L.S. Starrett Co., Athol, MA.

2 and 3 were used to calculate G.

TORSIONAL YIELD STRENGTH

A yield point was determined by using a static torsion test apparatus with the specimen clamped between the rotating fixture below, and the torsional load cell above (Figure 8). A torque (T) vs. angular deflection (ø) tracing was generated for each specimen during torsional loading and unloading on the Instron machine. A series of fifteen specimens was tested for each wire type and size with gradually increasing maximum torque (T_{Max}) values covering both the elastic and plastic areas of behavior. Again, the output was collected digitally on the Commodore computer, and transferred to the IBM PC/XT where it was displayed for analysis. A basic program called <TORSION> was developed that allowed four cursors to be overlaid on the output screen (Figure 9). The first cursor marked the peak of the curve, thereby defining T_{Max} for that specimen. The second, third, and fourth cursors were placed at the start rotation, reverse rotation, and return to baseline points, respectively. <TORSION> then used an algorithm to calculate the areas under the loading and unloading portions of the curve. The amounts of energy loss (loading area - unloading area) were compared to the amounts of elastic energy recovered (unloading area) and the torque (T) that resulted in 5, 10, and 20% energy loss was

determined. After the shape factors (k_1)[27] (Table II) and wire dimensions of d, b, and h (in.) were determined (Figure 1), the maximum shear stresses (τ_{Max})* were calculated from the T values via the formulas:[27]

for circular cross sections,

$$\tau_{Max}\ (psi) = \frac{16 \cdot T}{d^3}\ , \qquad (4)$$

and for rectangular cross sections,

$$\tau_{Max}\ (psi) = \frac{k_1 \cdot T}{h \cdot b^2}\ . \qquad (5)$$

τ_{ys} was defined as the τ_{Max} for 5, 10, and 20% energy loss.

ELASTIC PROPERTY RATIOS

These τ_{ys} and G values were used to determine the torsional Elastic Property Ratios (EPR's) in accordance with the relationships developed by Kusy and Greenberg.[10] Torsional comparisons of rectangular wire x with rectangular wire y were done using the following relationships:

---

* The maximum shear stress occurs at the outer fibers of a round wire and the fibers at the middle of the longest side of a rectangular wire.

stiffness ratio,

$$\left[\frac{G(bh)^3}{(b^2+h^2)}\right]_y \left[\frac{(b^2+h^2)}{G(bh)^3}\right]_x ,$$

strength ratio,

$$\frac{(\tau_{ys}hb^2)_y}{(\tau_{ys}hb^2)_x} ,$$

and range ratio,

$$\frac{\left[\frac{\tau_{ys}(b^2+h^2)}{Gbh^2}\right]_y}{\left[\frac{\tau_{ys}(b^2+h^2)}{Gbh^2}\right]_x} .$$

The EPR's were graphically displayed using a nomogram format.[28]

CHAPTER 3

RESULTS

WIRE DIMENSIONS

The cross-sectional wire dimensions which were measured by the digital micrometer are given in Table IV.

All measurements except two were less than the nominal dimensions. The h dimension of the .019x.025" S.S. averaged 0.02514", and the b dimension of the .019x.025" ß-Ti was 0.01916". All measurements were within 0.0005" of nominal size except the h dimension of .017x.025" ß-TI which was 0.00065" less than nominal.

The variability of the round wires of all materials was less than the rectangular wires. The standard deviations for round wire ranged from 0.00004-0.00007", while the rectangular wires varied from 0.00008-0.00018".

LOAD CELL CALIBRATION

The load cell proved to provide accurate and linear torque measurements from 0-1 kg-cm. The results were independent of load cell orientation.

SHEAR MODULUS

The G results for the inverted pendulum are given in Table V, column 2. The rectangular S.S. values were nearly the same (9.81 and 9.82 Msi), but were less than the .018" round (10.58 Msi). Among the ß-Ti wire sizes, all shear moduli were in the range of 4.22-4.42 Msi. The Ni-Ti rectangular wire G values (2.11 and 2.13 Msi) were less than the round wire values (2.96 Msi), a pattern similar to the S.S. The standard deviations for all inverted pendulum testing ranged from 0.02-0.15 Msi.

The results from the hanging pendulum (Table V, column 3) showed the same pattern as the inverted configuration. S.S. and Ni-Ti alloys had round wire values greater than rectangular wire values. The ß-Ti results all fell within a limited range. The variability was also similar to the inverted results with standard deviations ranging from 0.01-0.08 Msi.

Figure 10 shows a comparison of the inverted pendulum and hanging pendulum results. The two tests gave similar results, so the results were averaged and the mean values given in Table V, column 4.

The values listed in Table V, column 2, are arithmetic means of the inverted pendulum results. The inverted pendulum results were also analyzed by a least squares regression method by plotting $1/P^2$ against k/I_{mass}, where k represents the geometric variables of wire cross-section

and length (Figure 11). Plotting values in this way makes the slope of the regression line equal to G. The difference in G between round and rectangular wires for S.S. and Ni-Ti, noted above, again became apparent. Therefore, round and rectangular wires were analyzed independently for these two materials. The coefficients of correlation (r) for these regression lines were all greater than 0.999. The results of this least squares regression method (cf. Figure 11) were similar, but not identical, to the arithmetic mean method.

TORSIONAL YIELD STRENGTH

A log-log plot of energy loss and elastic energy recovered against the maximum shear stress (τ_{Max}) yielded two relatively straight lines (Figure 12). As a result, all torsional yield strength results were subject to geometric regression analysis and equations derived in the form:

$$\text{Energy(loss or recovered)} = A \cdot \tau_{Max}^{B},$$

where A and B are constants. The r's for the energy loss regressions were all greater than 0.92 and most greater than 0.95. All elastic energy regressions had r's greater than or equal to 0.99. The result was an energy loss equation and an elastic energy recovered equation for each

wire size and type. Figures 13-15 show these functions graphically for S.S., ß-Ti, and Ni-Ti, respectively. The two equations,

$$\text{Energy recovered} = A1 \cdot \tau_{Max}^{B1},$$

and

$$\text{Energy loss} = A2 \cdot \tau_{Max}^{B2},$$

can then be solved simultaneously and arranged to define the τ_{Max} at which a certain percent energy loss occurs.

$$\tau_{Max} = \left[\frac{100 \cdot A2}{\text{Percent} \cdot A1}\right] \wedge \left[\frac{1}{B1 - B2}\right]$$

Table VI, columns 2-4, give torsional yield strength results for 5, 10, and 20% energy loss, and Figures 16-18 show these values graphically for the three alloys. The round wire values for S.S. and ß-Ti are less than rectangular values for the same materials. Rectangular Ni-Ti values are much less than round wire values.

CHAPTER 4

DISCUSSION

WIRE DIMENSIONS

Only the .019x.025" ß-Ti was larger than nominal size in the b dimension, or that dimension normally restricted by bracket slot size. Even in this case, it would not result in a wire insertion problem because bracket slot sizes of .019" are not used. It would, however, affect the amount of activation needed to engage the orthodontic bracket for torsional tooth movement.

The dimensions for T.M.A. in this study compare favorably with those reported by Kusy and Stush[9] (cf. Table IV, in parentheses). The .017x.025" results were nearly identical with standard deviations slightly higher for this study. The .019x.025" measurements are slightly greater in the b dimension and slightly less in the h dimension, but it is interesting that the cross-sectional areas (b x h) are nearly the same. The wire specimens used in this study were probably formed from the same sized round wire stock, but not rolled quite as flat during the forming process. The .018" T.M.A. wires measured 2% larger in this study than the measurements reported by Kusy and Stush.

The dimensions reported for Nitinol by Kusy and Stush were up to 3% smaller than those reported in this study. The variability reported was similar, however.

The small differences from those previously reported may be due to either actual sample differences or technique differences. The fact that there wasn't a consistent, systematic difference in the measurements may discount a technique difference. On the other hand, because the micrometer "saw" a larger portion of the wire, it may have been more susceptible to surface irregularities or to imperceptible bends or twists in the wire.

SHEAR MODULUS

Once the necessary apparatus was assembled, the torsion pendulum provided an efficient, reproducible method for measuring the shear modulus of orthodontic archwires. Since the two configurations of the pendulum produced comparable results, future studies could select either method for more comprehensive testing. Due to the minimal effect of tension in the hanging configuration, the use of a lightweight hanging pendulum would probably give adequate results without extrapolation. Figure 7 shows a typical regression plot (.017x.025" S.S.) where an error in G of <0.1% occurs for every 100 grams of pendulum weight. Even the steepest regression slopes, which were for nickel-titanium wires, resulted in errors of <0.4% in G for each 100 grams of pendulum weight.

The values of G for S.S. wires were 5-10% below the standard literature value of 11.2 Msi.[29,30] One

explanation of this difference would be a clamping error as described by Nederveen and Tilstra.[22] To explore this possibility, a 6" length of each wire type and size (except the .018" Ni-Ti wire, which was limited to a 2" length) was tested at 9 different clamping lengths (1-5", in 0.5" increments). These tests were done with a lightweight pendulum in the hanging configuration as described earlier. The value of P^2 was plotted as a function of length (analogous to Figure 2 of ref. 19), and a linear regression line calculated (Figure 19). The point at which this line intercepted the abscissa was defined as the negative of the length correction (ΔL) needed to pass the regression line through the origin. ΔL was then expressed as a percentage of the 2" specimen length (cf. Table V, column 6) and a percent change in the modulus determined (cf. Table V, column 7). As will be seen shortly, not only does this methodology give values which closely approximate literature values, but the correction also removes the apparent difference in modulus between round and rectangular S.S. wires. This procedure of length correction for clamping error deserves consideration for future investigations whether done by either dynamic or static apparatus.

Table VII compares shear modulus results (experimental and corrected) to literature values for similar, non-orthodontic alloys[29,30,31,32,33,34] and to theoretical

values. The theoretical relationship G=E/[2(1+v)], in which E= Young's modulus and v= Poisson's ratio, assumes an isotropic material.[35] Values for E were taken from recent studies on orthodontic wires tested in bending[4,5,9] and values of v taken from engineering references and articles.[29,30,31,32,34] The literature values for non-orthodontic alloys (column 4) generally agreed with the theoretical calculations (column 7) except for Ni-Ti where the literature values were slightly higher than theoretical values. After correction, all G values closely approximated the theoretical values, and all but the rectangular Ni-Ti fell within the range of non-orthodontic literature values (cf. columns 3, 7, and 4). As stated earlier, these rectangular wires were obtained in straight lengths, while the Ni-Ti round wire samples were available only as preformed arches. Although only the straight part of the preformed arch was utilized for testing, the heat treatment used to set the arch form likely altered the microstructure of the entire wire. Further evidence of this difference was exhibited by the pseudoelastic appearance of the rectangular Ni-Ti wires in the yield tests which was not evident in the preformed, round wires (Figure 20). For this reason, values of G obtained for the preformed Ni-Ti (here, the .018" wire) should be used to calculate the EPR's of rectangular Ni-Ti, since they best represent the clinically used alloy.

TORSIONAL YIELD STRENGTH

The yield determination raised the recurring problem of defining a clinically significant yield criteria. The 10% energy loss criteria was selected for use in calculating EPR's because it was a minimal, yet detectable, amount of energy loss. To put it in perspective, when some previous S.S. tension data were analyzed by energy loss, an 0.1% offset roughly corresponded to a 20% energy loss as described in this study. The 10% loss point is thought to closely define the end of the elastic region with little permanent deformation occurring.

The pseudoelastic behavior noted in the rectangular Ni-Ti wires proved to be another troublesome problem in defining a yield point. Because of the energy lost to phase transformation in the elastic range (Figure 20, top), application of the energy loss criteria provides very low values of τ_{ys} (13-17 ksi for 10% loss, cf. Table VI, column 3) which would be inappropriate for calculating EPR's. In an attempt to get realistic τ_{ys} values to compare the rectangular Ni-Ti to the other wires, an alternative approach was tried. The Johnson Elastic Limit (JEL) defines the yield strength as a 50% change in slope (i.e., "A" versus "B" in Figure 20).[36] Three samples of each wire size and type were run in the static torsion apparatus with a gauge length of 1" (Figure 8). The paper chart

recordings of the torque vs. angular deflection were collected, and the yield strength via the JEL was defined. For the rectangular Ni-Ti, only the slope change beyond the pseudoelastic region was considered. The JEL values were consistently higher than the 10% energy loss values because a higher degree of permanent deformation was acceptable (cf. Figure 20 and Table VI, columns 3 and 7). The relationship of the rectangular Ni-Ti values to the others were more sensible now, however; as in the other two alloys the rectangular values were greater than the round wire values. In calculating the EPR's, the JEL yield strength values should be considered, too.

Table VI also shows the experimental τ_{ys} values compared to theoretical values of τ_{ys} calculated from the yield strength in tension (σ_{ys}) according the relationship,[37] $\tau_{ys}=0.577\sigma_{ys}$ where values of σ_{ys} have been taken from the orthodontic literature.[2,3,21] None of the experimental τ_{ys} values (columns 2-4) appear to be in general agreement with the theoretical values (column 6). This is due to the fact that the yield point has been defined in many ways or that the torsional yield strength is susceptible to change based on heat treatments or the extent of cold working. Kusy and Stush[9] found that titanium alloys don't follow the expected relationship between yield strength in tension and ultimate tensile strength. In spite of these difficulties, the τ_{ys} value

should affect the calculated EPR least because G is, among the material parameters, the largest contributor to the EPR's.

ELASTIC PROPERTY RATIOS

The rectangular wire EPR's shown in Table VIII were calculated three ways using different values for G and τ_{ys}. A .017x.025" S.S. was used as a reference wire for all calculations.

The first values used experimental G results (Table V, column 4) and 10% energy loss τ_{ys} values (Table VI, column 3). τ_{ys} values for the preformed .018" Ni-Ti were used for the rectangular Ni-Ti calculations for reasons mentioned previously. From the first entries in Table VIII, one sees that no wire has a strength less than an .017x.025" S.S. and that only an .019x.025" S.S. has less range. The Ni-Ti wires have ranges 5.19-5.33 times that of the reference wire. These EPR's may be unrealistic because the G values are uncorrected and the τ_{ys} values are estimated from the round wire for the Ni-Ti.

The second set of EPR's (Table VIII, numbers in parentheses) uses the length corrected G values and the JEL torsional yield strength values (cf. last columns of Tables V and VI, respectively). In this case, .018" values were not used for rectangular Ni-Ti wires. These substitutions result in little change in the EPR's for S.S. and Ni-Ti.

There is a large change in the EPR's for ß-Ti with strength, stiffness and range values all being less. The largest differences are in the strength and range values; they are due to the use of JEL τ_{ys} values. As mentioned previously, the JEL accepts a greater amount of plastic deformation than the 10% energy loss criteria. Because the formability of ß-Ti is less than that of S.S., the slope of the torque-angular deflection tracing changes more rapidly. The JEL is based on this slope change and therefore the JEL for ß-Ti is relatively less than that of S.S.. To reiterate, the difference in the torsional strength of S.S. and ß-Ti is largely due to behavior beyond the proportional limit; thus, there is little difference in 10% non-elastic values but, a distinct difference in JEL values. The rectangular Ni-Ti is not affected by this same phenomena. A relative increase in τ_{ys} using the JEL is seen in these wires because it is able to disregard the pseudoelastic behavior.

The third set of EPR's, for Ni-Ti only (Table VII, numbers in brackets), uses the same approach as the second set but substitutes G values obtained for .018" round wires for the rectangular calculations. This is an attempt to make the EPR's more clinically applicable. As mentioned before, it is thought that the difference in G between round and rectangular Ni-Ti in this study is due to the heat process involved in setting the arch form. Because

most clinicians obtain Ni-Ti wires in the preformed arches, the higher G values for preformed arches were used. Compared to either previous set of calculations, this substitution results in a relative increase in stiffness and a concomitant decrease in range.

Those EPR values thought to be most clinically applicable (the last value listed for each wire size and type in Table VIII) were illustrated in a nomogram in Figure 21 along with a nomogram illustrating the theoretical EPR's published by Kusy and Greenberg in 1981.[10] The S.S. lines are nearly identical in the two nomograms which is to be expected because a S.S. wire is used as the reference. Although the differences are small, the nomogram from this study shows β-Ti with greater strength and stiffness but less range than the theoretical nomogram. This is due to a combination of higher G values and relatively higher strength values than theoretically anticipated. The greatest discrepancies are noted when comparing the Ni-Ti lines of the two nomograms. More range, but less stiffness and strength were calculated theoretically than were seen experimentally. Among the fundamental material properties, the largest difference was found in the experimental value of G which was 50% greater than theoretically expected. The τ_{ys} values also contributed to the difference because Ni-Ti was theoretically to have only 80% the strength of S.S.

although experimentally it proved to be about equal. Overall, the ranking of the EPR's of these wires remained constant, however.

CHAPTER 5

SUMMARY

The torsional elastic properties of stainless steel (S.S.), beta titanium (ß-Ti), and nickel-titanium (Ni-Ti) archwires were determined. One round (.018") and two rectangular (.017x.025" and .019x.025") wires sizes were investigated for each alloy.

The shear modulus (G) was determined dynamically using a torsion pendulum. Two configurations of the pendulum were used and found to give nearly identical results. A correction factor for clamping error was determined for each wire size and type. G values for S.S. were found to be 11.02-11.33 Msi, for ß-Ti were 4.29-4.41 Msi, and for Ni-Ti were 2.29-3.08 Msi. The large variation in Ni-Ti values was accounted for by the heat treatment used to set the arch form in the round Ni-Ti wires tested.

The torsional yield strength (τ_{ys}) was first described by using a 10% energy loss criteria. This method proved useful for S.S., ß-Ti, and preformed Ni-Ti wires, but was not applicable for the rectangular Ni-Ti wires because of their apparent pseudoelastic behavior. Using this method, all values were about 100 ksi except for .018" S.S. (51 ksi) and the rectangular Ni-Ti (13 and 17 ksi). Subsequently, the τ_{ys} was defined using the Johnson Elastic

Limit (JEL) which proved useful for those wires which displayed pseudoelastic behavior. Using the JEL, τ_{ys} values were generally higher because, by definition, a greater amount of permanent deformation was accepted.

Elastic property ratios were calculated using the G and τ_{ys} values deemed most clinically meaningful. These were then displayed in a nomogram format and compared with previous theoretical work.

CONCLUSIONS

1. The torsion pendulum proved an efficient, reproducible apparatus to measure the shear modulus of orthodontic archwires.

2. The energy loss criteria for torsional yield strength determination proved useful for classically behaving alloys; but an alternative, such as the Johnson Elastic Limit, was required for specimens displaying apparent pseudoelastic behavior.

3. The testing methods provided sufficient information to allow the calculation of elastic property ratios (EPR's) for predicting the torsional behavior of orthodontic archwires.

4. When the present experimental results were compared to previous theoretical EPR calculations, certain differences were noted. These differences were greatest for the nickel-titanium alloys and showed a relative decrease in range, and an increase in stiffness and strength.

5. Further testing using these methods is indicated to comprehensively describe archwire behavior in torsion.

APPENDICES

APPENDIX A

Preliminary shear modulus (G) testing was done with a static torsion apparatus (Figure 8). Gauge lengths (L) of 1-4" were used. Chart tracings were made on the Instron machine of torque (T) versus angular deflection (ø). The slope of the straight-line portion of these tracings (T/ø) was used to determine G from the relationship:

$$\phi = \frac{T \cdot L}{J \cdot G},$$

or,

$$G = \frac{T}{\phi} \cdot \frac{L}{J},$$

where J = the polar area moment of inertia.

The following results were obtained.

Wire Type and Size		Experimental G (Msi)
S.S.	.016"	9.31-11.7
	.020"	9.63-10.6
	.017x.025"	8.37-10.2
	.019x.025"	8.60-10.7
	.021x.025"	8.18-10.2
β-Ti	.018"	3.73-5.27
	.019x.025"	3.52-4.21
Ni-Ti	.017x.025"	1.56-2.21

APPENDIX B

Preliminary testing of the torsion pendulum was done on round wire samples of carbon steel, stainless steel, copper, and brass. The gauge lengths used were 3" and 5". No correction was made for clamping errors. Testing was done in both the inverted and hanging configurations (Figures 4 and 6, respectively).

The following results were obtained.

Wire Type and Size	Experimental G (Msi)	Literature G (Msi)
Carbon Steel .020"	11.05-11.32	12.5
Stainless Steel .020"	10.67-11.00	11.2
Copper .020"	6.51-6.70	6.4
Brass .025"	5.23-5.35	5.6

BIBLIOGRAPHY

1. Burstone CJ: Variable-modulus Orthodontics. Am J Orthod 80:1-16, 1981.

2. Kusy RP, Stevens LE: Triple-Stranded Stainless Steel Wires - Evaluation of Mechanical Properties and Comparison with Titanium Alloy Alternatives. Angle Orthod 57:18-32, 1980.

3. Kusy RP, Dilley GJ: Elastic Modulus of a Triple-stranded Stainless steel Arch Wire via Three- and Four-point Bending. J Dent Res 63:1232-1240, 1984.

4. Kusy RP: unpublished data.

5. Asgharnia KA, Brantley WA: Comparison of Bending and Tension Tests for Orthodontic Wires. Am J Orthod 89:228-236, 1986.

6. Yoshikawa DK, Burstone CJ, Goldberg AJ, Morton J: Flexure Modulus of Orthodontic Stainless Steel Wires. J Dent Res 60:139-145, 1981.

7. Goldberg AJ, Vanerby R, Burstone CJ: Reduction in Modulus of Elasticity in Orthodontic Archwires. J Dent Res 56:1227-1231, 1977.

8. Drake SR, Wayne DM, Powers JM, Asgar K: Mechanical Properties of Orthodontic Wires in Tension, Bending, and Torsion. Am J Orthod 82:206-210, 1982.

9. Kusy RP, Stush AM: Geometric and Material Parameters of a Nickel-Titanium and a Beta Titanium Orthodontic Arch Wire Alloy. Dent Mat, in press.

10. Kusy RP, Greenberg AR: Effects of Composition and Cross-section on the Elastic Properties of Orthodontic Archwires. Angle Orthod 51:325-341, 1981.

11. Thurow, RC: Edgewise Orthodontics. ed. 4, St Louis, 1981, The C. V. Mosby Company, pp. 33-38 and pp. 329-334.

12. New American Dental Association Specification No. 32 for Orthodontic Wires Not Containing Precious Metals. JADA 95:1169-1171, 1977.

13. Steyn CL: Measurements of Edgewise Torque in Vitro. Am J Orthod 71:565-573, 1977.

14. Wagner JA, Nikolai RJ: Stiffness of Incisor Segments of Edgewise Arches in Torsion and Bending. Angle Orthod 55:37-50, 1985.

15. Kusy RP: Comparison of Nickel-titanium and Beta Titanium Wire Sizes to Conventional Orthodontic Archwire Materials. Am J Orthod 79:625-629, 1981.

16. Clark WA, Plehn B: Materials Testing and Heat Treating. New York, 1942, Harper and Brothers Publishers, pp. 12-15.

17. Liddicoat RT, Potts PO: Laboratory Manual of Materials Testing. New York, 1952, The MacMillan Company, chapter X.

18. 1975 Book of ASTM Standards. Philadelphia, 1975, American Society for Testing and Materials, section E143-E161.

19. Boyer HE, Gall TL: Metals Handbook Desk Edition. Metals Park, OH, 1985, American Society for Metals, pp. 3436-3438.

20. Andreasen GF, Morrow RE: Laboratory and Clinical Analysis of Nitinol Wire. Am J Orthod 73: 142-151, 1978.

21. Zimmerman RD: A Torsional Comparison of Nitinol and Stainless Steel Orthodontic Archwires. M.S. Thesis Univ. of Iowa, 1980.

22. Nederveen CJ, Tilstra JF: Clamping Corrections for Torsional Stiffness of Prismatic Bars. J Phys D: Appl Phys 4:1661-1667, 1971.

23. Nielsen LE: Mechanical Properties of Polymers. New York, 1962, Reinhold Publishing Corporation, chapter 7.

24. Neilsen LE: A Recording Torsion Pendulum for the Measurement of the Dynamic Mechanical Properties of Plastics and Rubbers. The Review of Scientific Instruments 22:690-693, 1951.

25. Heijboer J: The Torsion Pendulum in the Investigation of Polymers. Polymer Engineering and Science 19:664-675.

26. Braden M, Stafford GD: Viscoelastic Properties of Some Denture Base Materials. J Dent Res 47:519-523, 1968.

27. Cernica JN: Strength of Materials. New York, 1966, Holt, Rinehard, and Wilson, Inc., p. 131.

28. Kusy RP: On the Use of Nomograms to Determine the Elastic Property Ratios of Orthodontic Arch Wires. Am J Orthod 83:374-381, 1983.

29. Source Book on Stainless Steels. Metals Park, OH, 1976, American Society for Metals, pp. 95-96.

30. Ledbetter HM: Sound Velocities and Elastic Constants of Steels 304, 310, and 316. Metal Science 14:595-596, 1980.

31. Collings EW: The Physical Metallurgy of Titanium Alloys. Metals Park, OH, 1984, American Society for Metals, pp. 116-118 and pp. 149-159.

32. Torok E, Simpson JP: Dynamic Elastic and Damping Properties of some Practical Ti-Base Alloys. In Titanium '80 Proceedings of the Fourth International Conference on Titanium. Vol 1, Kyoto, Japan, 1980.

33. Mercier O, Melton KN: Theoretical and Experimental Efficiency of the Conversion of Heat into Mechanical Energy Using Shape Memory Alloys. J Appl Phys 52:1030-1037, 1981.

34. Cross WB: Nitinol Characterization Study. NTIS #N269-36367, p. 3, 1969.

35. Sines G: Elasticity and Strength. Boston, 1969, Allyn and Bacon, Inc., pp. 156-157.

36. Fett GA: Induction Case Depths for Torsional Applications. Metal Progress 12:49-52, 1985.

37. Shigley JE: Mechanical Engineering Design, New York, 1963, McGraw-Hill Book Company, Inc., pp. 291-292.

TABLES

Table I

ALLOYS TESTED

Alloy	Code	Product
Stainless Steel	S.S.	Standard™ [a]
Beta Titanium	β-Ti	T.M.A.™ [b]
Nickel-Titanium	Ni-Ti	Nitinol™ [a]

[a] Unitek Corporation, Monrovia, CA.
[b] Ormco Corporation, Glendora, CA.

Table II

SHAPE FACTORS FOR EQUATIONS (3) and (5)

Ratio h/b [a]	Shape Factor k_1	Ratio h/b [a]	Shape Factor μ
1.0	4.81	1.00	2.249
1.5	4.33	1.20	2.658
2.0	4.07	1.40	2.990
3.0	3.75	1.60	3.250
4.0	3.55	1.80	3.479
6.0	3.34	2.00	3.659

[a] Ratio of height to base for rectangular wires (cf. Figure 1).

Table III

Pendulums Used for Shear Modulus Testing

Wire Type and Size (in.)	Pendulum polar mass moment of Inertia (I_{mass}) (gm-cm^2)						
	467	711	1047	1817	2309	4600	9348
S.S.							
.018	I[a]	I	I H[b]	I		I	
.017x.025			I	I	I H	I	I
.019x.025			I	I	I H	I	I
B-Ti							
.018	I	I	I H	I	I		
.017x.025	I	I	I H	I	I		
.019x.025		I	I H	I	I	I	
Ni-Ti							
.018	I	I	I H	I	I		
.017x.025	I	I	I H	I	I		
.019x.025	I	I	I H	I	I		

[a] Pendulums used in the inverted configuration denoted with an I.

[b] Pendulums used in the hanging configuration denoted with an H.

Table IV

MEASURED WIRE DIMENSIONS

Wire Alloy and Nominal Size (in.)	d (in.)	b (in.)	h (in.)
Stainless Steel			
.018	0.01786 ±0.00004[a]		
.017x.025		0.01687 ±0.00009	0.02493 ±0.00010
.019x.025		0.01894 ±0.00008	0.02514 ±0.00012
Beta Titanium			
.018	0.01756 ±0.00004 (0.01722 ±0.00010)[b]		
.017x.025		0.01689 ±0.00013 (0.01681 ±0.00009)	0.02435 ±0.00014 (0.02434 ±0.00008)
.019x.025		0.01916 ±0.00014 (0.01887 ±0.00009)	0.02460 ±0.00018 (0.02475 ±0.00007)
Nickel-Titanium			
.018	0.01776 ±0.00007 (0.01749 ±0.00016)		
.017x.025		0.01690 ±0.00009 (0.01643 ±0.00004)	0.02456 ±0.00012 (0.02450 ±0.00022)
.019x.025		0.01891 ±0.00013 (0.01837 ±0.00007)	0.02477 ±0.00014 (0.02437 ±0.00006)

[a] Mean ± one standard deviation.
[b] Dimensions in parentheses were previously reported by Kusy and Stush[9].

Table V

SHEAR MODULUS (G) VALUES AND CLAMPING CORRECTIONS

Wire Alloy and Size (in.)	Inverted[a] G Msi (GPa)	Hanging[b] G Msi (GPa)	Mean G Msi (Gpa)	Length Correction[c] ΔL (in.)	Length Correction ΔL/L·100 (%)	Corrected G Msi (GPa)
Stainless Steel						
.018	10.58±0.10 [d] (72.95±0.69)	10.71±0.08 (73.85±0.55)	10.65 (73.43)	0.07	3.5	11.02 (75.98)
.017x.025	9.81±0.15 (67.64±1.03)	9.89±0.05 (68.19±0.34)	9.85 (67.92)	0.30	15.0	11.33 (78.12)
.019x.025	9.82±0.09 (67.71±0.62)	9.87±0.03 (68.05±0.21)	9.85 (67.92)	0.29	14.5	11.28 (77.78)
Beta Titanium						
.018	4.24±0.04 (29.23±0.28)	4.26±0.05 (29.37±0.34)	4.25 (29.30)	0.05	2.5	4.36 (30.06)
.017x.025	4.42±0.02 (30.48±0.14	4.41±0.01 (30.41±0.07)	4.42 (30.48)	-0.06	-3.0	4.29 (29.58)
.019x.025	4.22±0.03 (29.10±0.21)	4.18±0.05 (28.82±0.34)	4.20 (28.96)	0.10	5.0	4.41 (30.41)
Nickel-Titanium						
.018	2.96±0 03 (20.41±0.21)	3.00±0.03 (20.69±0.21)	2.98 (20.58)	0.07	3.5	3.08 (21.24)
.017x.025	2.13±0.03 (14.69±0.21)	2.20±0.04 (15.17±0.28)	2.17 (14.96)	0.19	9.5	2.38 (16.41)
.019x.025	2.11±0.03 (14.55±0.21)	2.16±0.02 (14.89±0.14)	2.14 (14.76)	0.14	7.0	2.29 (15.79)

[a] cf. Figure 4.
[b] cf. Figure 6.
[c] cf. Figure 19.
[d] Mean ± one standard deviation.

Table VI

TORSIONAL YIELD STRENGTH (τ_{YS}) VALUES

Wire Alloy and Size (in.)	τ_{ys} by Energy Loss[a] 5% ksi (MPa)	10% ksi (MPa)	20% ksi (MPa)	Literature Values σ_{ys} ksi (MPa)	Theoretical Values $\tau_{ys}=0.577\sigma_{ys}$ ksi (MPa)	Johnson Elastic Limit[b] ksi (MPa)
Stainless Steel						
.018	36 (248)	51 (352)	73 (503)	185[4] (1276)	107 (738)	115 (793)
.017x.025	74 (510)	98 (676)	132 (910)	240-280[5] (1655-1930)	138-162 (952-1117)	210 (1448)
.019x.025	67 (462)	90 (621)	119 (821)	↓	↓	216 (1489)
Beta Titanium						
.018	85 (586)	95 (655)	105 (724)	76[9]-170[5] (524-1172)	44-98 (303-676)	110 (758)
.017x.025	83 (572)	100 (690)	120 (827)	99[9]-140[5] (683-965)	57-81 (393-558)	138 (952)
.019x.025	93 (641)	106 (731)	121 (834)	98[9]-190[5] (676-1310)	57-110 (393-758)	137 (945)
Nickel-Titanium						
.018	96 (662)	114 (786)	135 (931)	94[9]-100[5] (648-690)	54-58 (372-400)	148 (1020)
.017x.025	7 (48)	17 (117)	39 (269)	42[9]-78[5] (290-538)	24-45 (165-310)	216 (1489)
.019x.025	4 (28)	13 (90)	36 (248)	57[5]-68[9] (393-469)	33-39 (228-269)	223 (1538)

[a] cf. Figure 9.
[b] cf. Figure 20.

Table VII

SHEAR MODULUS (G) VALUES

Wire Alloy and Size (in.)	Current Study: Exp.[a] G Msi (GPa)	Current Study: Corrected[b] G Msi (GPa)	Literature Values: G Msi (GPa)	Literature Values: E[c] Msi (GPa)	Literature Values: v[d]	Theoretical: G= E/[2(1+v)] Msi (GPa)
Stainless Steel						
.018	10.65 (73.43)	11.02 (75.98)	11.2[29,30] (77.2)	28.4[4] (195.8)	0.29[30]-0.30[29]	10.9-11.0 (75.2-75.8)
.017x.025	9.85 (67.92)	11.33 (78.12)		27.9-28.1[5] (192.4-193.7)		10.7-10.9 (73.8-75.2)
.019x.025	9.85 (67.92)	11.28 (77.78)				
Beta Titanium						
.018	4.25 (29.30)	4.36 (30.06)	3.9[31]-4.5[32] (26.8-31.0)	12.0[9]-12.3[5] (82.7-84.8)	0.29[32]-0.36[31]	4.4-4.8 (30.3-33.1)
.017x.025	4.42 (30.48)	4.29 (29.58)		9.5[9]-11.5[5] (65.5-79.3)		3.5-4.5 (24.1-31.0)
.019x.025	4.20 (28.96)	4.41 (30.41)		10.6[9]-13.8[5] (73.1-95.2)		3.9-5.3 (26.9-36.5)
Nickel-Titanium						
.018	2.98 (20.58)	3.08 (21.24)	2.9[33]-3.6[34] (20.0-24.8)	7.6[5]-7.7[9] (52.4-53.1)	0.33[34]	2.9 (20.0)
.017x.025	2.17 (14.96)	2.38 (16.41)		6.0[9]-7.4[5] (41.4-51.0)		2.3-2.8 (15.9-19.3)
.019x.025	2.14 (14.76)	2.29 (15.79)		5.4[9]-5.5[5] (37.2-37.9)		2.0-2.1 (13.8-14.5)

[a] cf. Table V, column 4.
[b] cf. Table V, column 7.
[c] E = Modulus of Elasticity = Young's Modulus.
[d] v = Poisson's Ratio.

Table VIII

TORSIONAL ELASTIC PROPERTY RATIOS
Reference wire: .017" x .025" Stainless Steel

Wire Alloy and Size (in.)	Stiffness	Strength	Range
Stainless Steel			
.017x.025	1.00[a] (1.00)[b]	1.00 (1.00)	1.00 (1.00)
.019x.025	1.33 (1.32)	1.17 (1.31)	0.88 (0.99)
Beta Titanium			
.017x.025	0.43 (0.37)	1.00 (0.64)	2.31 (1.76)
.019x.025	0.56 (0.51)	1.37 (0.83)	2.46 (1.63)
Nickel-Titanium			
.017x.025	0.22 (0.21) [0.27][c]	1.15 (1.02) [1.02]	5.33 (4.94) [3.82]
.019x.025	0.28 (0.26) [0.35]	1.45 (1.33) [1.33]	5.19 (5.09) [3.78]

[a] Standard ratios calculated using experimental shear modulus (G) values (cf. Table VII, column 2) and 10% energy loss τ_{ys} values (cf. Table VI, column 3). .018" Ni-Ti τ_{ys} values used for all Ni-Ti.

[b] Ratios in parenthesis use corrected G values (cf. Table VII, column 3) and Johnson elastic limit τ_{ys} determinations (cf. Table VI, column 7).

[c] Values of G from .018" preformed arches used in calculating EPR's, otherwise the same as b.

FIGURES

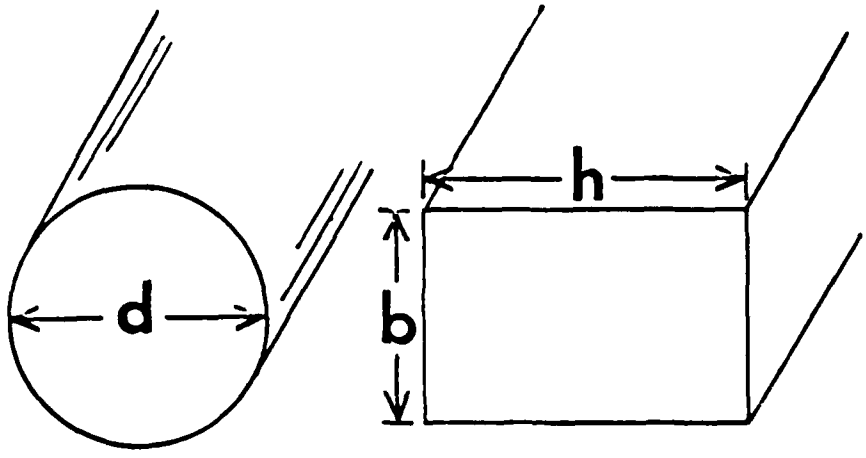

Figure 1 -- Cross-sectional archwire measurements. Diameter (d) for round wires, base (b) and height (h) for rectangular wires.

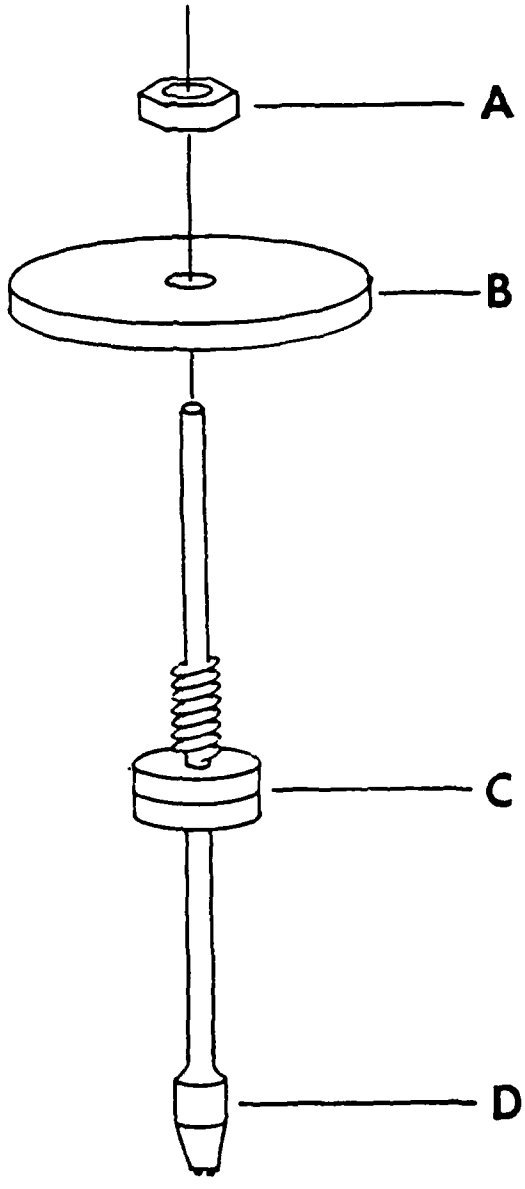

Figure 2 -- Exploded schematic of torsion pendulum.

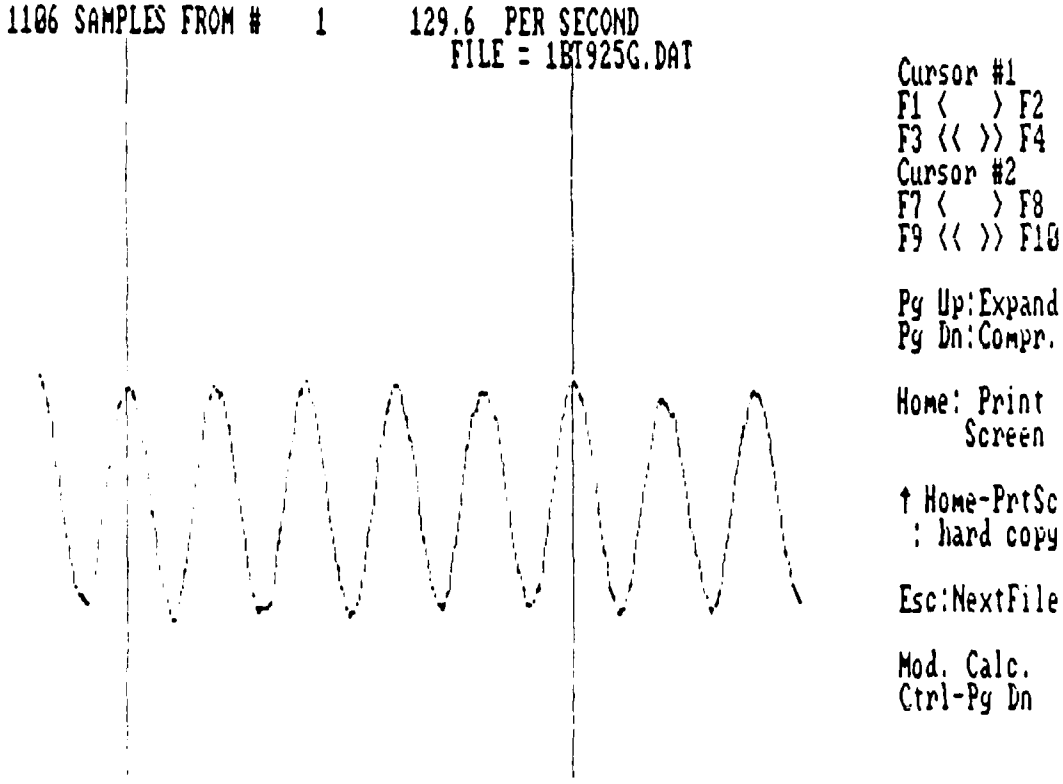

Figure 3 -- Computer screen from <PENDULUM> showing cursors in place over first five full oscillations.

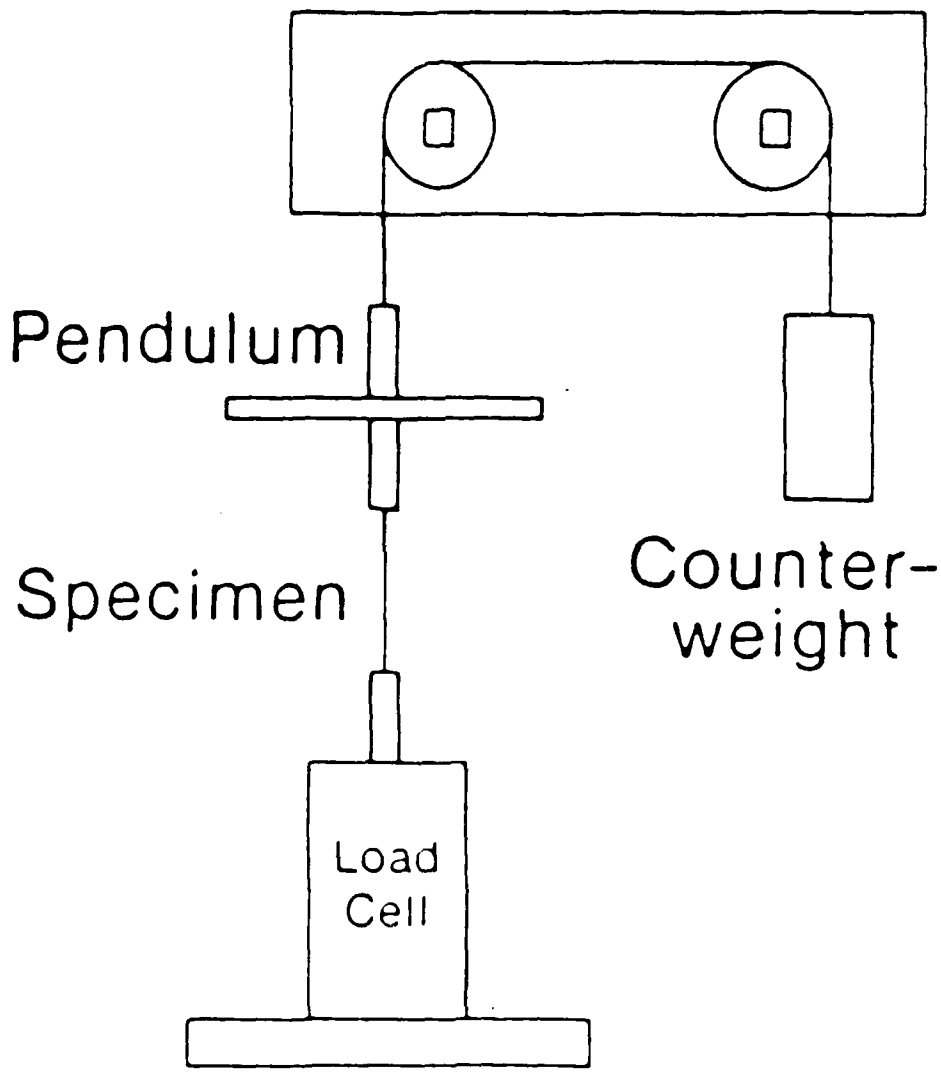

Figure 4 -- Inverted torsion pendulum configuration.

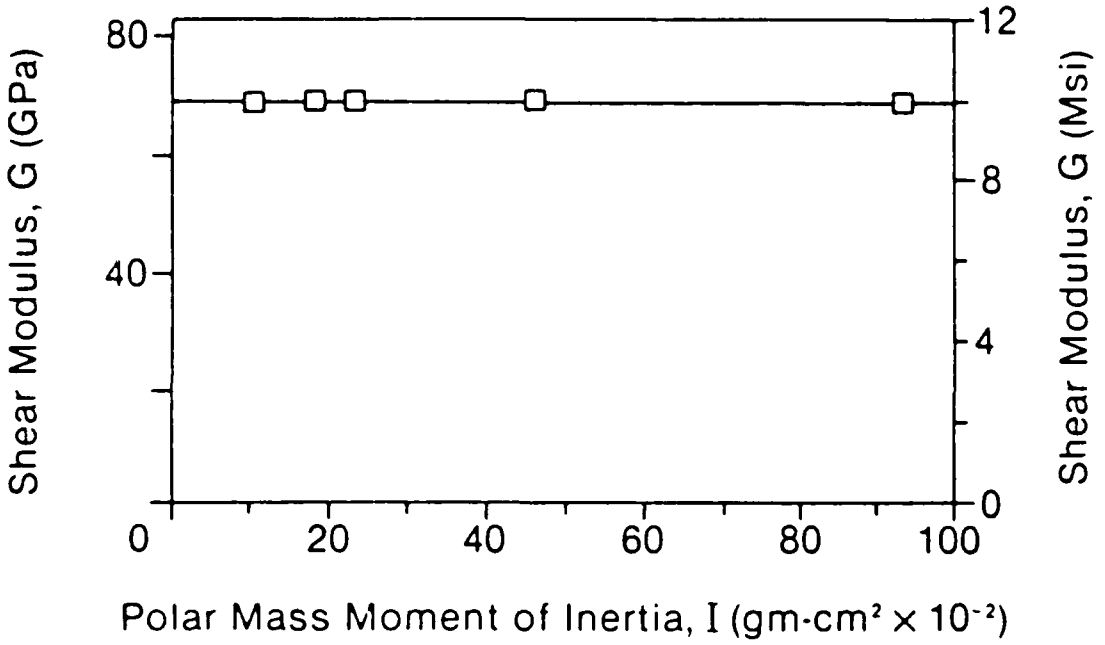

Figure 5 -- An example of stability of G with different I_{mass} pendulums for .017x.025" S.S.

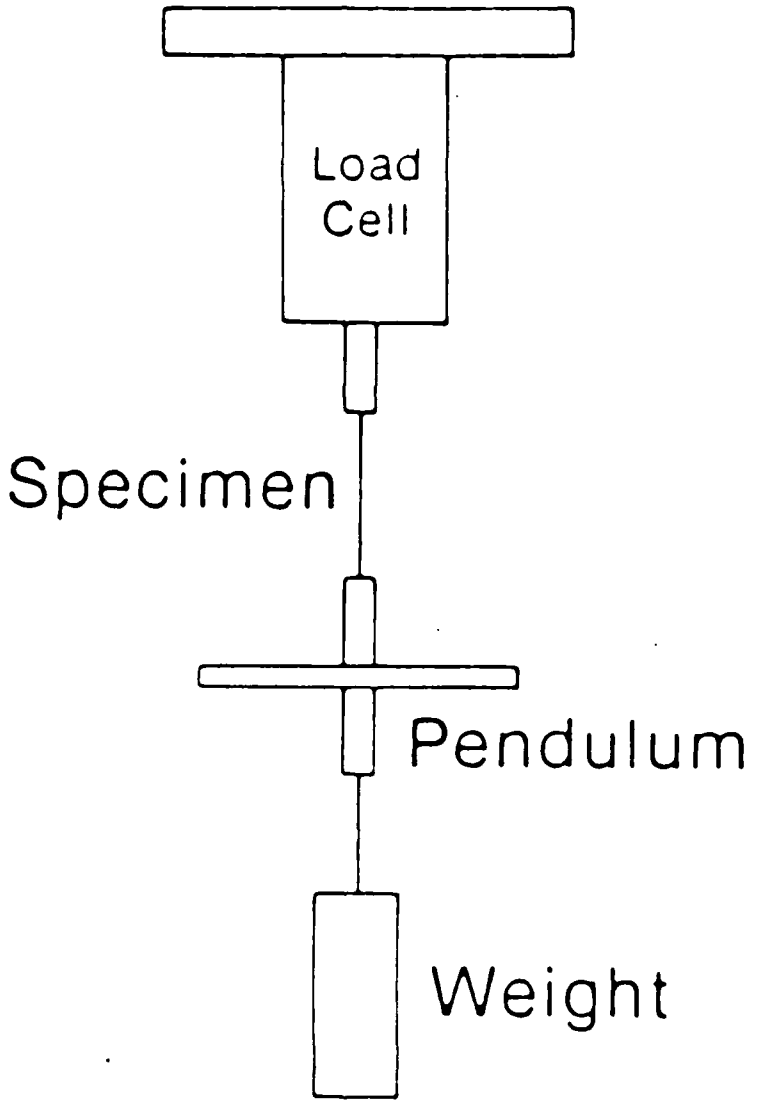

Figure 6 -- Hanging torsion pendulum configuration.

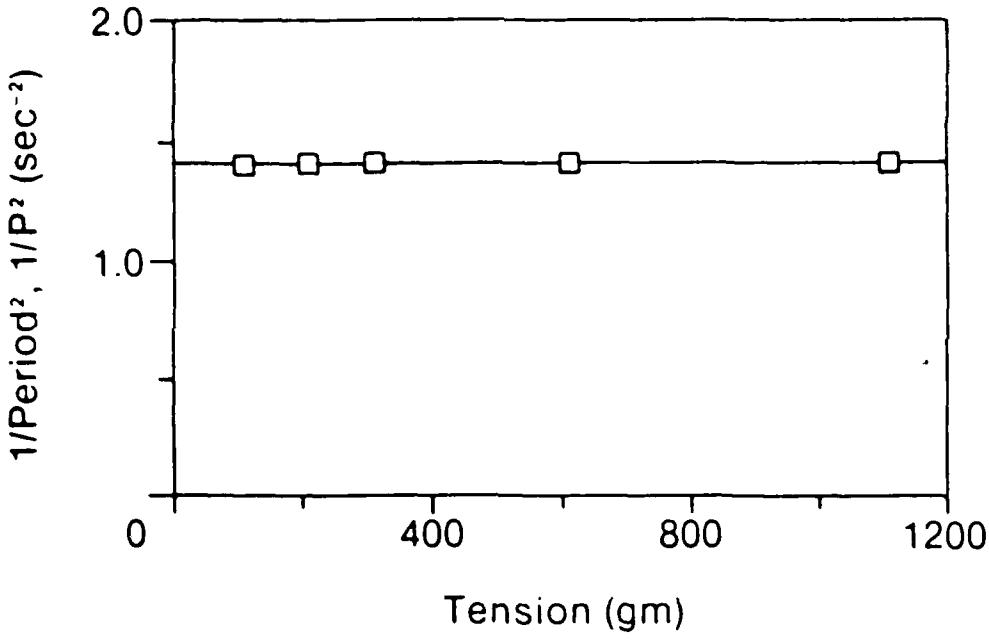

Figure 7 -- An example of regression plot for .017x.025" S.S. to determine P at zero tension with hanging configuration of the torsion pendulum. $1/P^2$ plotted against tension on pendulum (gm) for a constant I_{Mass}.

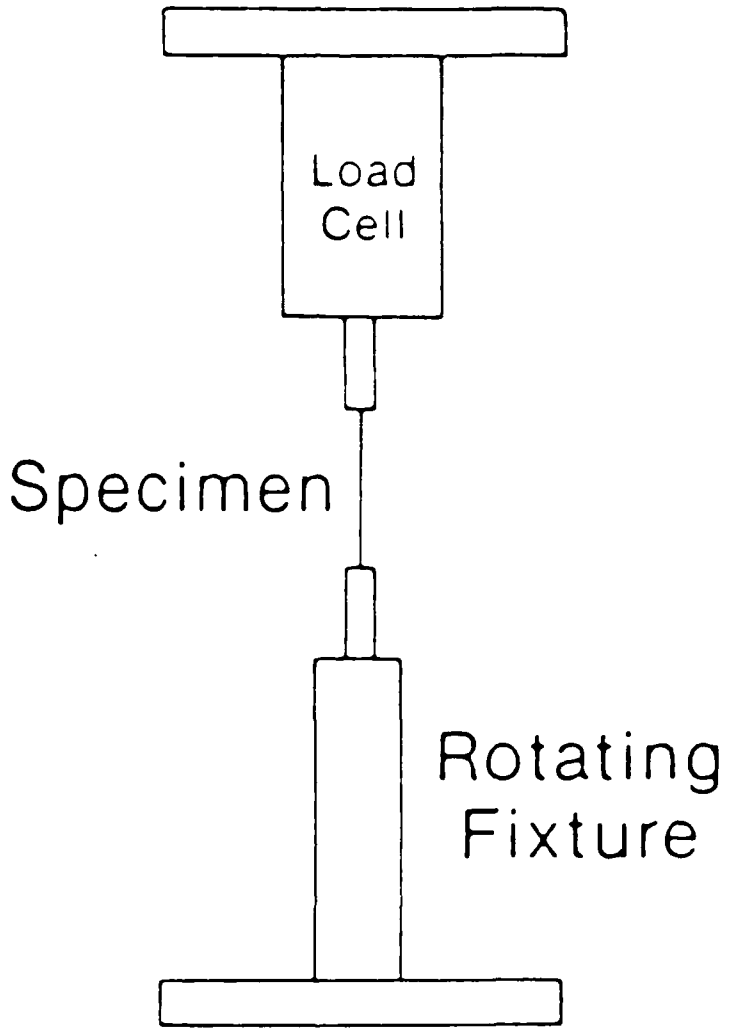

Figure 8 -- Static torsion apparatus.

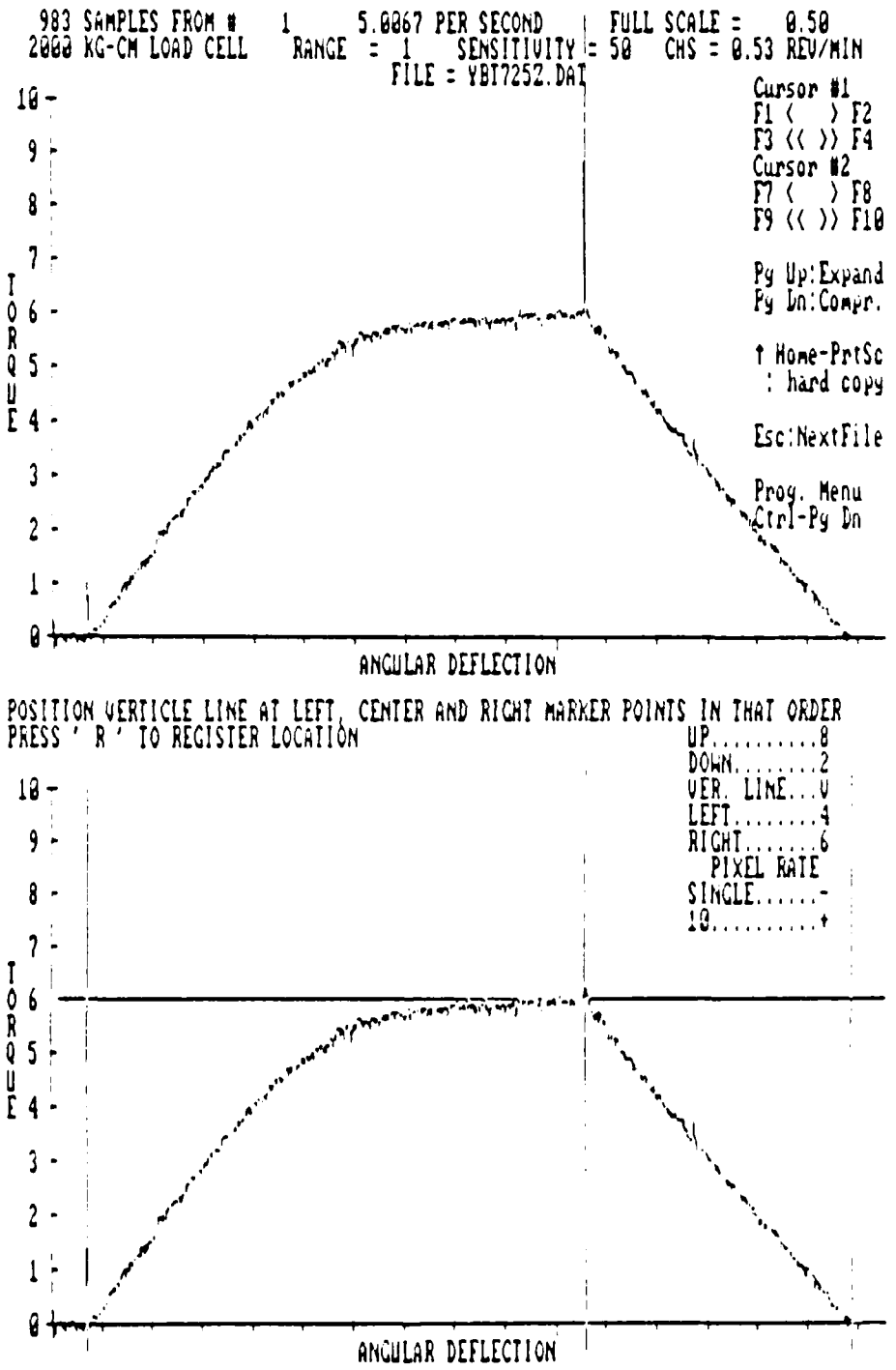

Figure 9 -- Two computer screens from <TORSION>. Top shows tracing before cursors are placed, and bottom show all four cursors positioned.

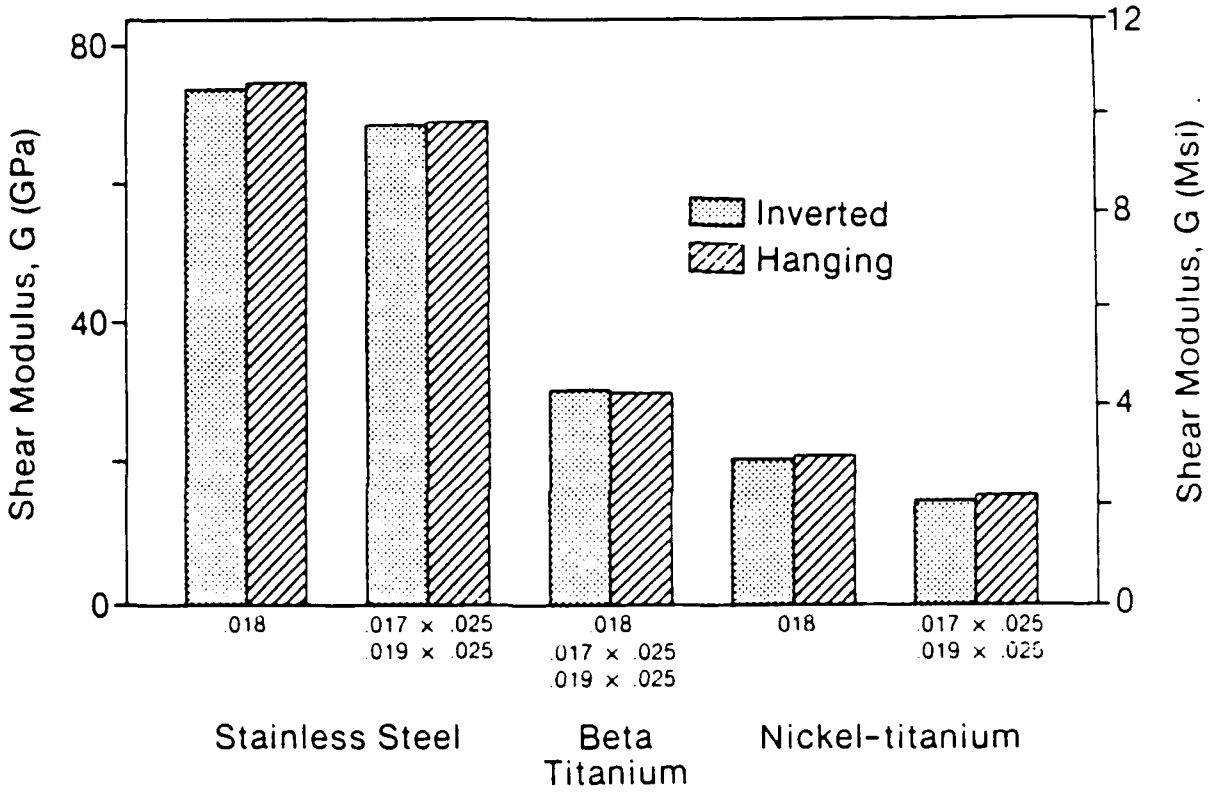

Figure 10 -- Bar graph comparing results of inverted and hanging pendulum tests.

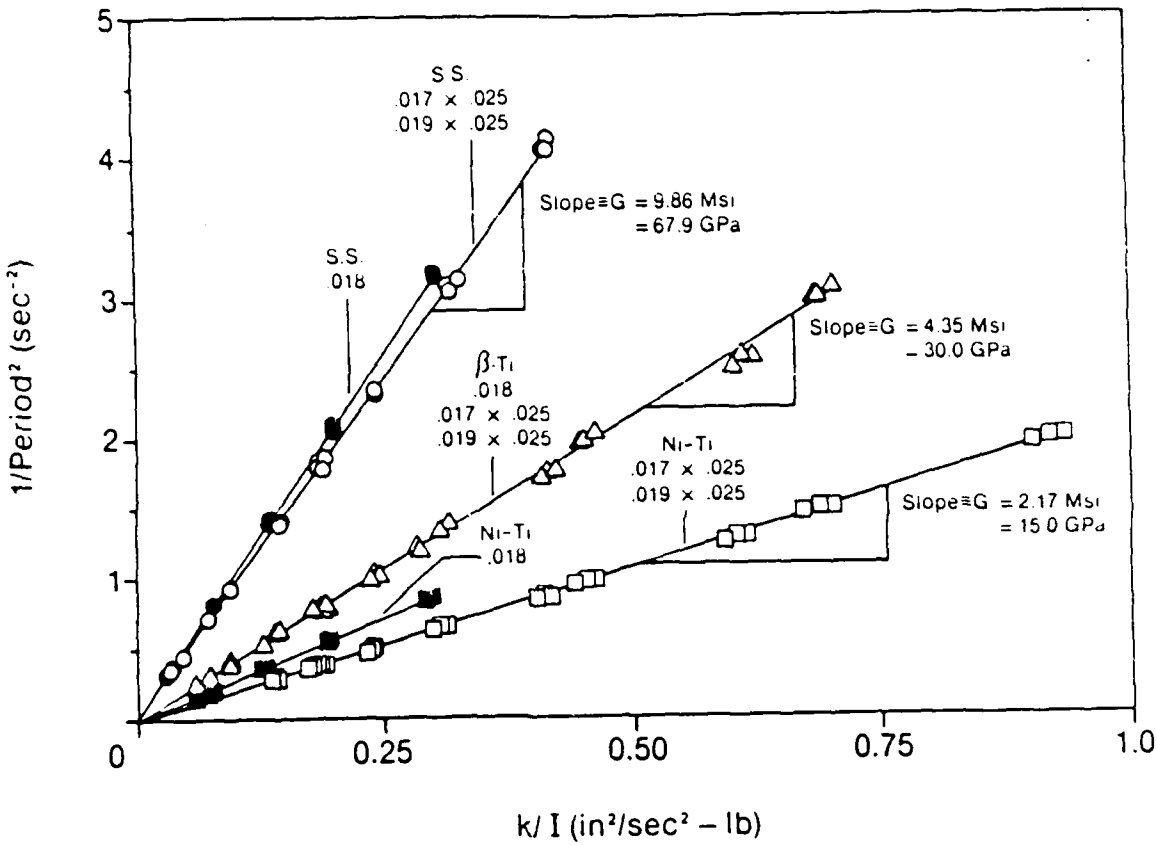

Figure 11 -- Plot of inverted pendulum data so that the slopes of the regression lines equal G. For circular cross-sections (eq. 2) $k=d^4/(.000355 \cdot L)$; whereas for rectangular cross-sections (eq. 3), $k=h \cdot b^3 \cdot \mu/(.0005588 \cdot L)$. The G's for the solid symbol regressions were: .018" S.S. =10.65 Msi, .018" Ni-Ti =2.98 Msi.

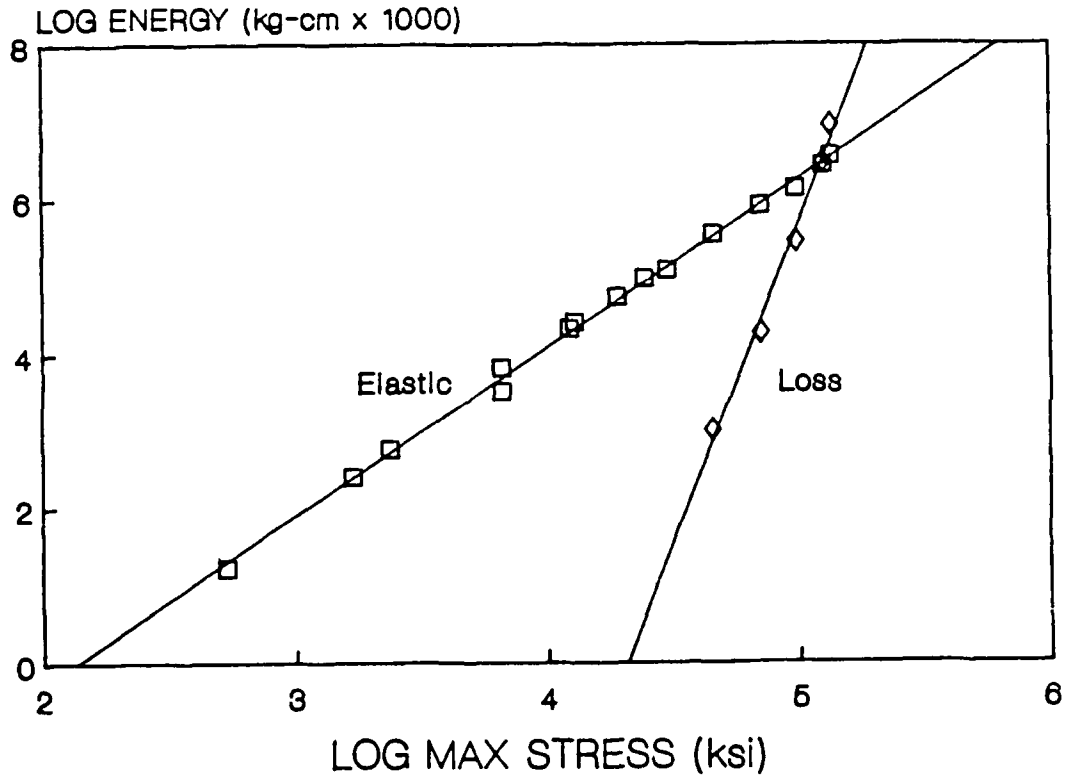

Figure 12 -- Example of log-log plot for elastic and non-elastic energy data from a sample of .019x.025" β-Ti. The straight-line plots led to the use of geometric regressions to describe the data.

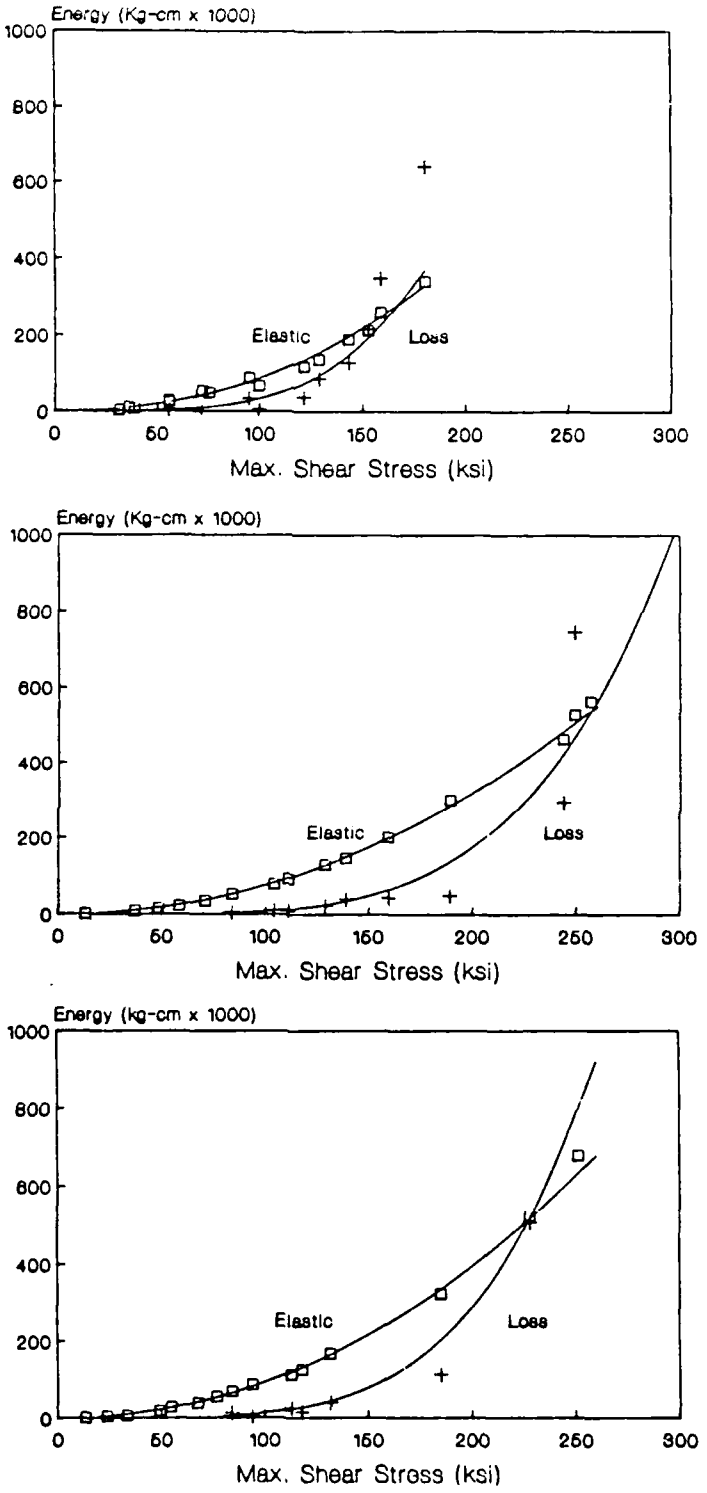

Figure 13 -- Stainless steel elastic and energy loss data with geometric regression curves. From top to bottom: .018", .017x.025", and .019x.025".

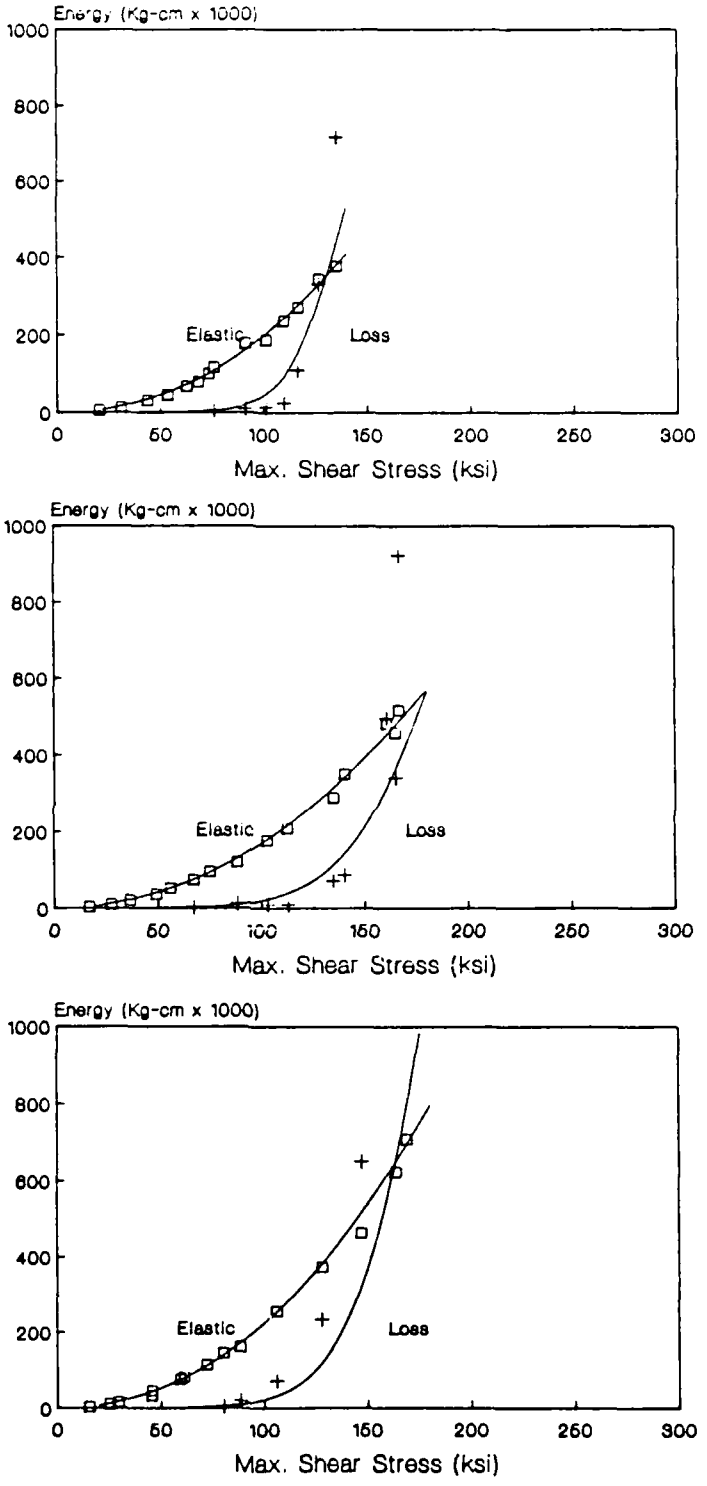

Figure 14 -- Beta titanium elastic and energy loss data with geometric regression curves. From top to bottom: .018", .017x.025", and .019x.025".

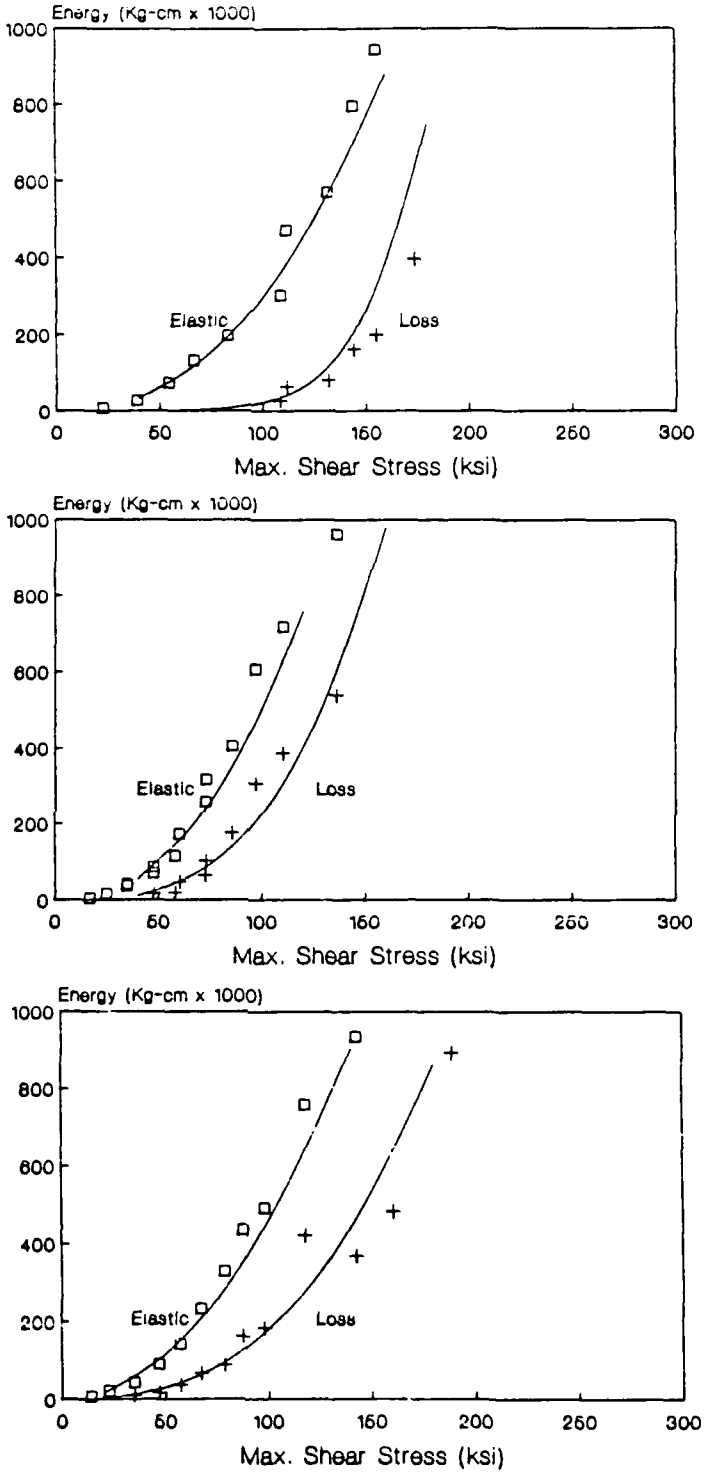

Figure 15 -- Nickel-titanium elastic and energy loss data with geometric regression curves. From top to bottom: .018", .017x.025", .019x.025".

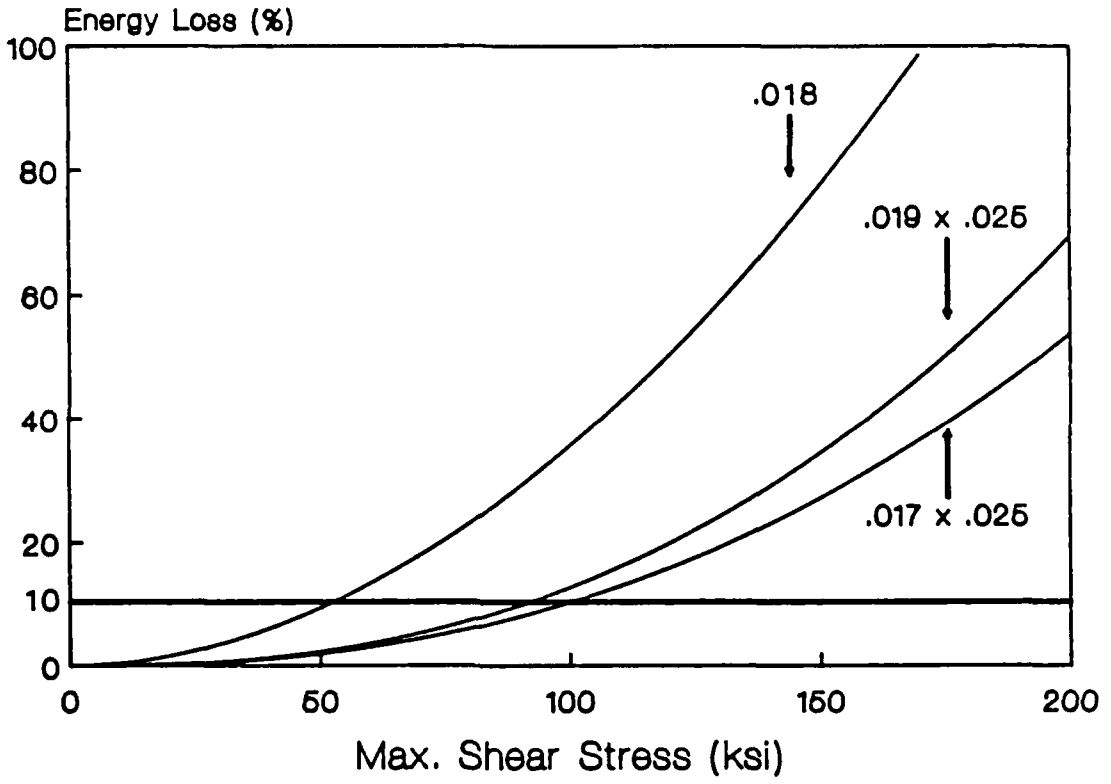

Figure 16 -- Stainless steel energy loss functions for .018", .017x.025", and .019x.025". Horizontal line drawn at the 10% level that was selected for describing τ_{ys}.

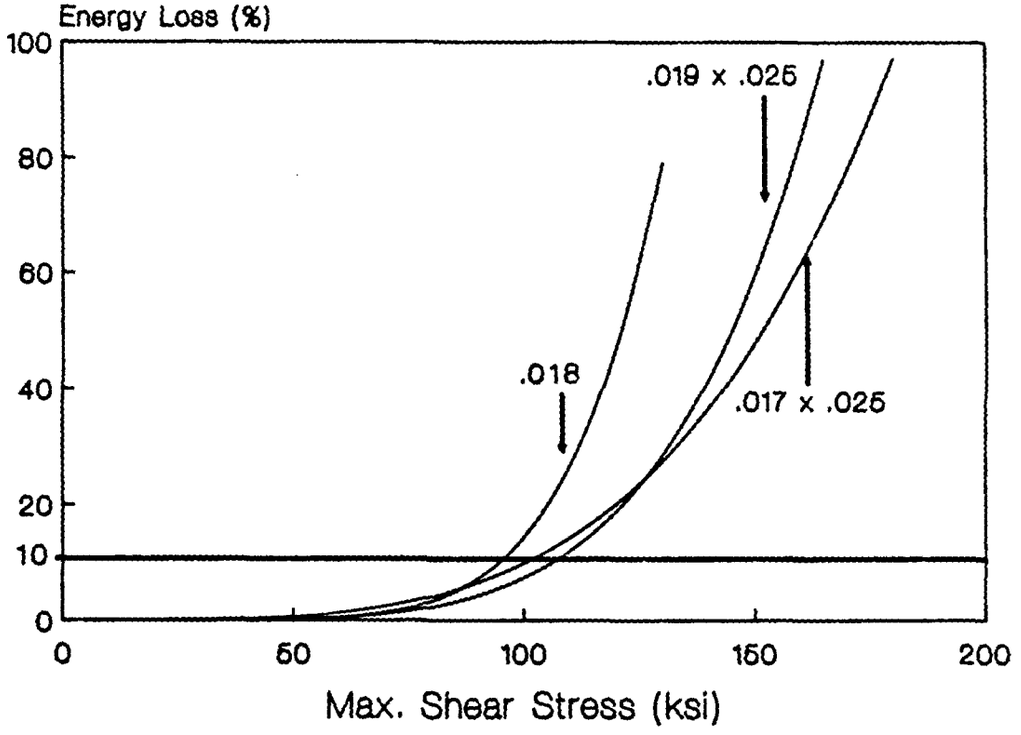

Figure 17 -- Beta titanium energy loss functions for .018", .017x.025", and .019x.025". Horizontal line drawn at the 10% level that was selected for describing τ_{ys}.

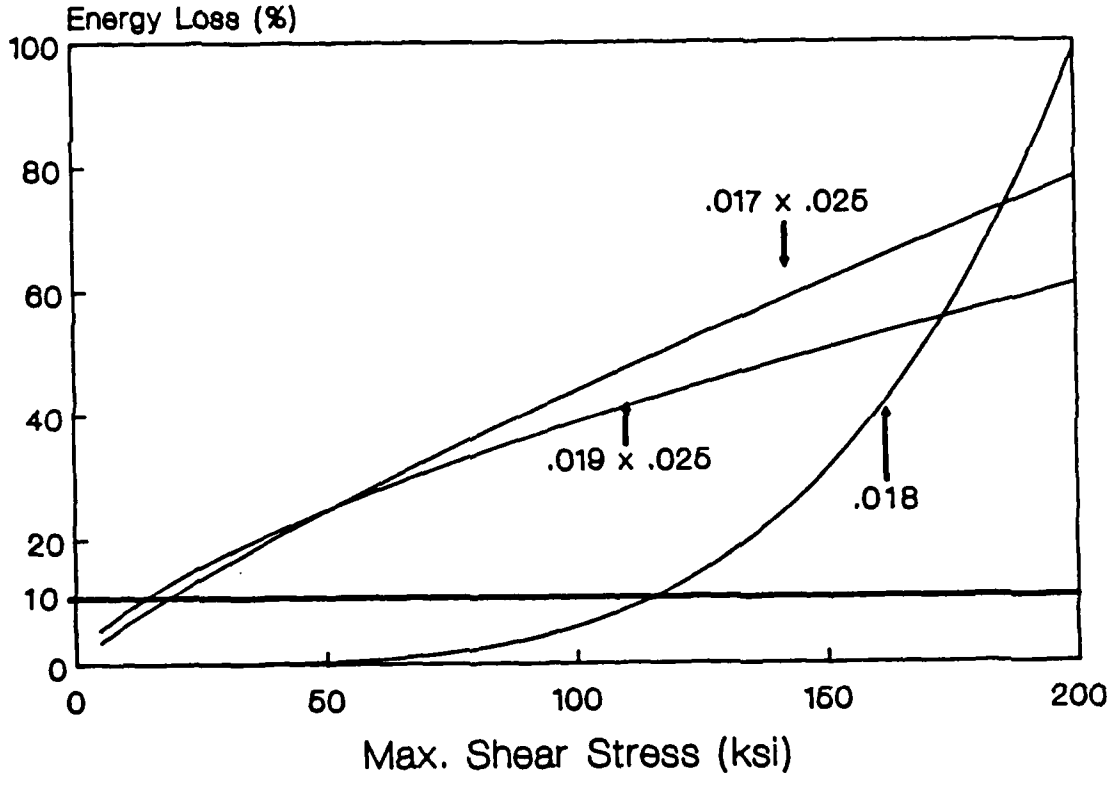

Figure 18 -- Nickel-titanium energy loss functions for .018", .017x.025", and .019x.025". Horizontal line drawn at the 10% level that was selected for describing τ_{ys}.

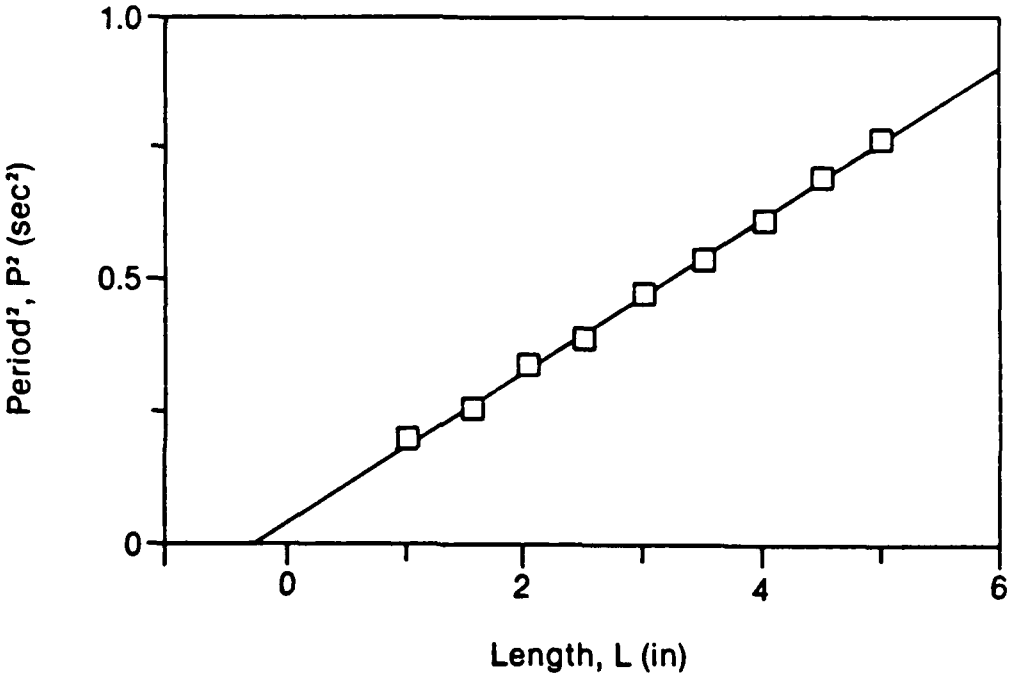

Figure 19 -- Length correction regression example for .017x.025" S.S. The regression line intercepts the abscissa at a point with the coordinates (- ΔL, 0), which in this case gives a ΔL = 0.30" (cf. Table V, column 5).

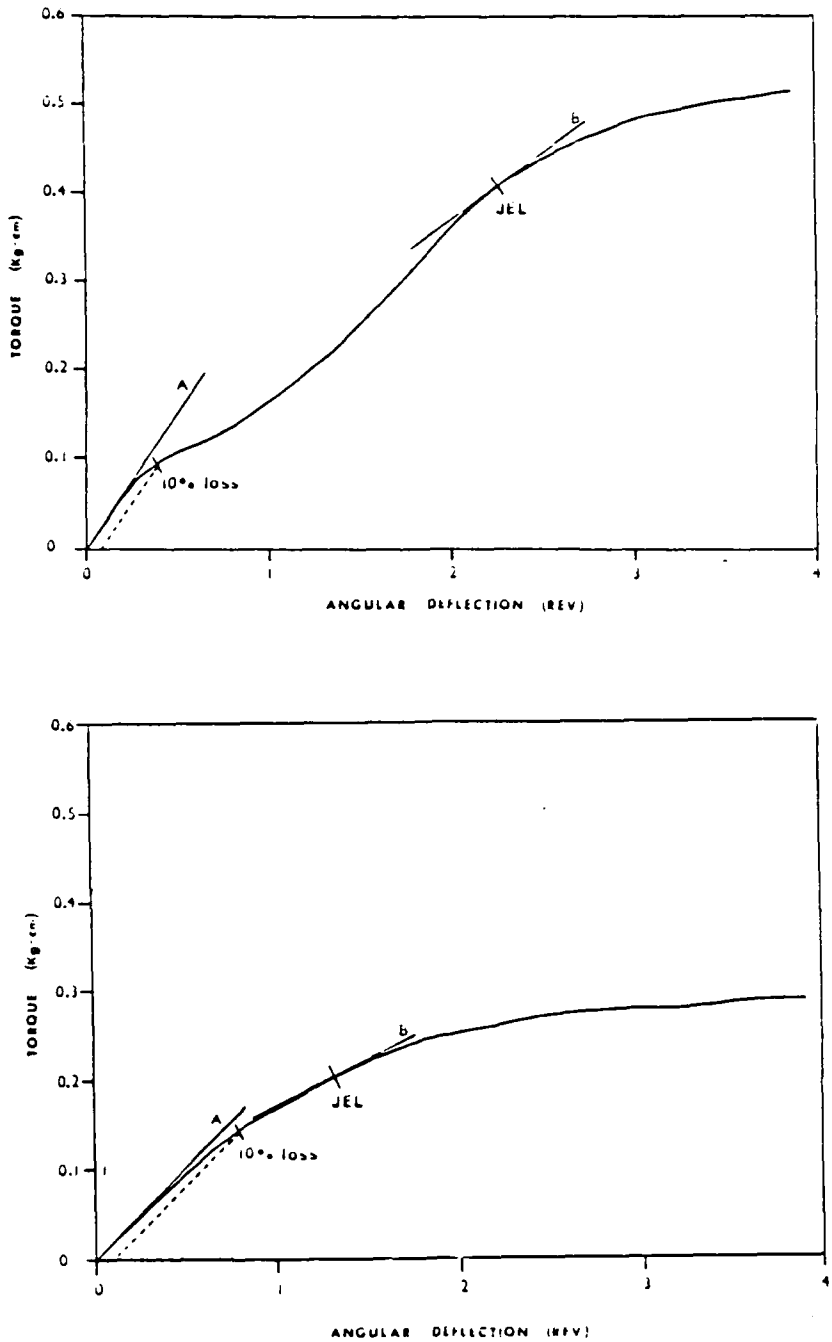

Figure 20 -- Torsional loading curves which were obtained for Ni-Ti in straight lengths (.017x.025", top) and in preformed arches (.018", bottom). The straight lengths demonstrated a degree of non-linear elasticity which made the 10% loss criteria inappropriate. As an alternative, the Johnson Elastic Limit (JEL) was determined as the point beyond the pseudoelastic region where the slope, B, was 50% of the initial slope, A.

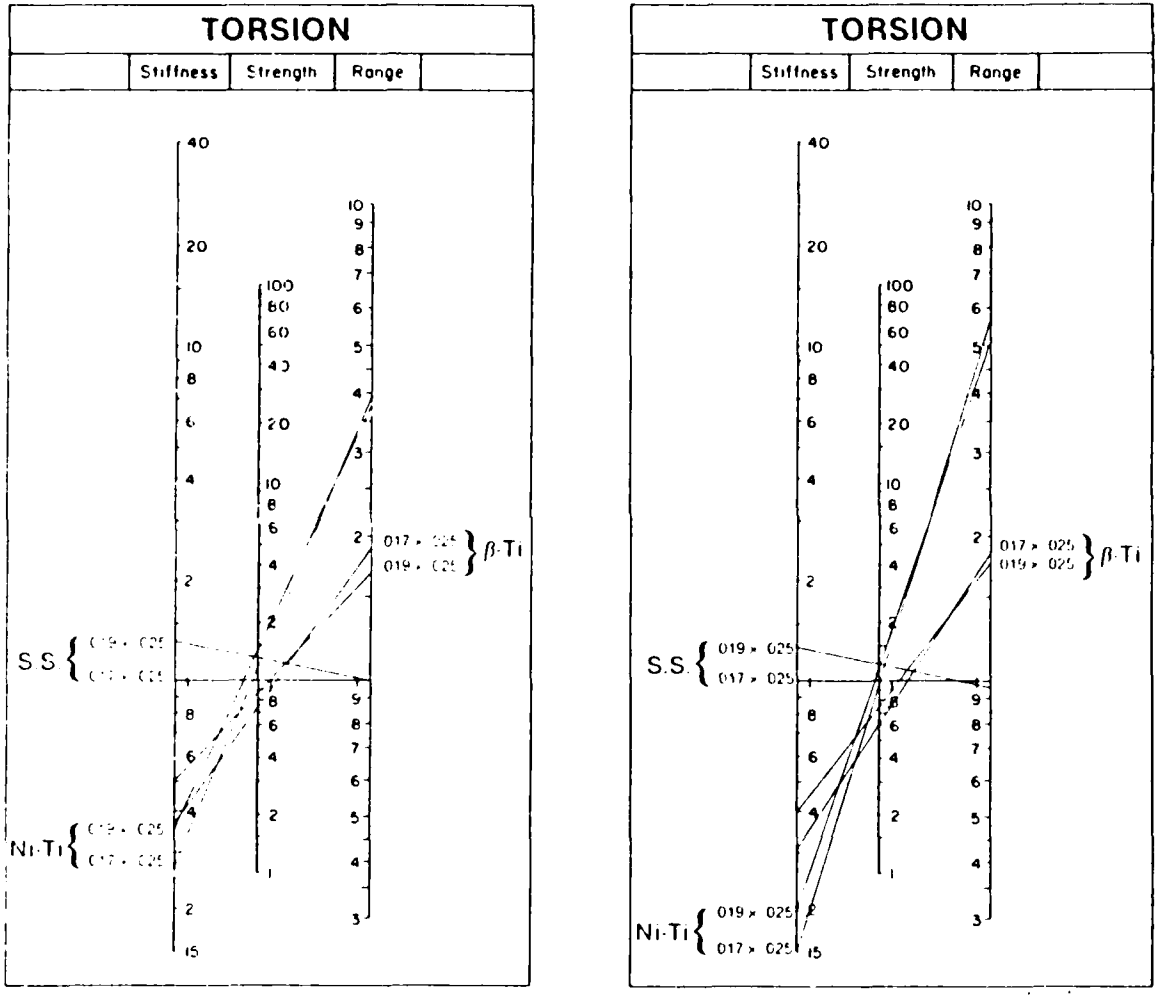

Figure 21 -- Nomograms depicting the elastic property ratios (EPR's) for this present experimental investigation (left) versus the previous theoretical study by Kusy and Greenberg[10] (cf. Table VIII).

END

DATE

FILMED

DEC.

1987